

Distributed Estimation via Network Regularization

Lingzhou Hong, Alfredo Garcia, and Ceyhun Eksin

Texas A&M University

Abstract

We propose a new method for distributed estimation of a linear model by a network of local learners with heterogeneously distributed datasets. Unlike other ensemble learning methods, in the proposed method, model averaging is done continuously over time in a distributed and asynchronous manner. To ensure robust estimation, a network regularization term which penalizes models with high local variability is used. We provide a finite-time characterization of convergence of the weighted ensemble average and compare this result to centralized estimation. We illustrate the general applicability of the method in two examples: estimation of a Markov random field using wireless sensor networks and modeling prey escape behavior of birds based on a real-world dataset.

Keywords: Ensemble learning, Federated Learning, Network Lasso, Markov Random Field, Stochastic Optimization

1 Introduction

The ever-growing size and complexity of data create scalability challenges for storage and processing. For example, in certain application domains, data cannot be stored or processed in a single location, due to geographical constraints or limited bandwidth. In such cases, a distributed architecture for data storage or processing relying on a network of interconnected computers not necessarily in the same physical location may be required. Since the datasets may not be independent or identically distributed, the quality of locally estimated models may vary significantly.

In a “divide and conquer” approach (see, e.g., [1], [2] and [3]) individual machines implement a particular learning algorithm to fit a model for their assigned data set and *upon each machine identifying a model*, an ensemble (or global) model is obtained by averaging individual models. Model averaging is an active area of research in statistics (see e.g. [4], [5]). A careful selection of weights for computing the average model ensures a reduction of estimation variance along with other desirable properties. Another relevant literature in machine learning pertains to *ensemble learning* (see, e.g., [6]) which refers to methods that combine different models into a single predictive model. For example, bootstrap aggregation (also referred to as “bagging”) is a popular technique for combining regression models from *homogeneously* distributed data. Next, there is literature on the optimal combination of forecasts (see [7] and [8]). Combining forecasts from different models can be shown to increase forecast robustness against measurement errors and model misspecification. For example, with heteroscedasticity, weights minimizing the sample mean square prediction error are of the form $\hat{\sigma}_i^{-2} / \sum_{j=1}^N \hat{\sigma}_j^{-2}$ where $\hat{\sigma}_i > 0$ is the estimated mean squared prediction error of the i -th model (see [8]). Federated Learning (FL) is a relatively new area of study (see, e.g., [9], [10], [11] and [12]), it learns a global model collaboratively over a large set of distributed nodes by exchanging parameters or gradients without integrating data. The Federated Multi-Task Learning (FMTL)

further reduces communication cost by allowing each node to learn a local model and only share its parameters with neighbors.

While a “divide and conquer” approach coupled with a model averaging step can significantly reduce computing time and lower single-machine memory requirements, it relies on a synchronized step (i.e., computing the ensemble average) which is executed *after all* machines have identified a model. Therefore, in a strict sense, there are no finite-time performance guarantees.

In this paper, we introduce a “divide and conquer” approach for learning linear models in which model averaging is done *continuously* over time in a distributed and asynchronous manner. In the proposed distributed scheme, each computer (or local learner) is assigned a dataset and *asynchronously* implements stochastic gradient updates based upon a sample (or a mini-batch sample). To ensure robust estimation, a network regularization term which penalizes models with high variability is used. Unlike other model averaging schemes based upon a synchronized step, we are able to provide finite-time performance guarantees for stochastic gradient descent.

Our distributed estimation scheme is equipped to deal with heterogeneous data sets with a graph-structure. Methods for processing data with graph-structure have been recently proposed (see, e.g., [13], [14] and [15]). In the Network Lasso method, local models are learned by optimizing a combination of model fit and a network regularization penalty. In these papers, it is assumed that data points are affected by independent and identically distributed noise. In contrast, our proposed network regularizer can be seen as an extension to Network Lasso for distributed linear model estimation with heterogeneous datasets exhibiting heteroscedasticity and correlation.

Though our scheme is similar to FL and FMTL in minimizing a weighted combination of loss functions and a regularization penalty. Unlike FL, we train personalized models for each node locally and asynchronously with low communication cost. Differently from FMTL, we are interested in training a global model, which is obtained by taking a weighted average of the parameters from local models while the performance is guaranteed by properly handling the heterogeneous data.

Due to heteroscedasticity and correlation, the centralized problem is a generalized least squares problem. Here, we approximate the generalized least squares problem whose solution requires the inversion of the covariance matrix of the linear model by the sum of weighted least squares problems with network regularization, which is a convex problem. Hence, our model and the algorithm relates to decentralized convex optimization [16–20] and the recent work on finding the best common linear model in convex machine learning problems [21]. Instead of finding a common linear estimate for all the nodes, we are interested in the weighted mean of the node estimates (ensemble mean) and its closeness to the solution of the generalized least squares problem. The distributed stochastic gradient descent algorithm converges to a different estimate for each node because each node has access to different data, i.e., solves its own weighted least squares problem with network regularization. The weight of the regularization term is a proxy for the correlation between the estimates of each node. As we show in Lemma 2 and in numerical experiments, by tuning the regularization weight, the ensemble mean estimate can be made close to the centralized solution.

The organization of the paper is as follows. In section 2, we describe the network structured distributed estimation and introduce the algorithmic framework for computing estimates. In section 3, we provide a characterization of convergence. In particular, we provide a finite-time characterization of convergence of the weighted ensemble average and compare this result to centralized estimation. Consistency of the ensemble estimator is also established. In section 4, we exemplify the applicability of the proposed method by considering a wireless sensor network (WSN) estimation of a Gaussian Markov random field (MRF), and by investigating the factors that determine birds escape behavior from predators.

2 Model

2.1 Setup

A large dataset with input $\mathbf{X} \in \mathbb{R}^{p \times d}$ and output $\mathbf{y} \in \mathbb{R}^p$ is divided into $N > 1$ disjoint subsets of the form $\{(\mathbf{X}_1, \mathbf{y}_1), \dots, (\mathbf{X}_N, \mathbf{y}_N)\}$, where $\mathbf{X}_i \in \mathbb{R}^{m \times d}$ ($m < p$) is the data on d features and $\mathbf{y}_i \in \mathbb{R}^m$ is the corresponding observation vector at data subset i .

We assume the model for each subset is as follows:

$$\mathbf{y}_i = \mathbf{X}_i \mathbf{w}^* + \varepsilon_i + \Lambda_i \xi, \quad i \in \mathcal{V} := \{1, \dots, N\}, \quad (1)$$

where $\mathbf{w}^* \in \mathbb{R}^d$ is the ground truth vector of coefficients, $\varepsilon_i \in \mathbb{R}^{m \times 1}$ is an *individual* noise vector specific to data subset i , and $\xi \in \mathbb{R}^{m \times 1}$ is a *common* noise which affects different subsets differently according to the matrices $\Lambda_i \in \mathbb{R}^{m \times m}$. In this paper, we consider Λ_i as a diagonal matrix with diagonal entries that are possibly different.

We assume the individual noise vector is zero-mean and independent across different subsets, i.e., $\mathbb{E}[\varepsilon_i \varepsilon_j^\top] = \mathbf{0}_{m \times m}$ for all i and $j \neq i$, and $\mathbb{E}[\varepsilon_i \varepsilon_i^\top] = \sigma_i^2 \mathbf{I}_m$. Also, $\mathbb{E}[\xi] = \mathbf{0}_m$ and $\mathbb{E}[\xi \xi^\top] = \mathbf{I}_m$. It follows the covariance matrix of the error term in the model for \mathbf{y}_i as

$$\Omega_i := \mathbb{E}(\varepsilon_i + \Lambda_i \xi)(\varepsilon_i + \Lambda_i \xi)^\top = \sigma_i^2 \mathbf{I} + \Lambda_i^2 \in \mathbb{R}^{m \times m}.$$

Since datasets are disjoint, we can express the entire dataset as $\mathbf{X} = [\mathbf{X}_1^\top, \dots, \mathbf{X}_N^\top]^\top$ and $\mathbf{y} = [\mathbf{y}_1^\top, \dots, \mathbf{y}_N^\top]^\top$ and assume the model for \mathbf{y} as:

$$\mathbf{y} = \mathbf{X} \mathbf{w}^* + \varepsilon + \Lambda \xi, \quad (2)$$

where $\Lambda = [\Lambda_1, \dots, \Lambda_N]^\top$ and $\varepsilon = [\varepsilon_1^\top, \dots, \varepsilon_N^\top]^\top$. The covariance matrix for the error term of \mathbf{y} is:

$$\Omega := \mathbb{E}(\varepsilon + \Lambda \xi)(\varepsilon + \Lambda \xi)^\top = \Sigma + \Lambda \Lambda^\top \in \mathbb{R}^{p \times p}.$$

where Σ is a block-diagonal matrix with the i -th block equal to $\sigma_i^2 \mathbf{I}_m$ and hence the noise across subsets is correlated. A centralized formulation of the generalized least squares consists of minimizing the following loss function over \mathbf{w} :

$$\mathcal{L}_c \triangleq \frac{1}{2} (\mathbf{y} - \mathbf{X} \mathbf{w})^\top \Omega^{-1} (\mathbf{y} - \mathbf{X} \mathbf{w}). \quad (3)$$

2.2 A Network of “Local” Learners

We shall assume each dataset $(\mathbf{X}_i, \mathbf{y}_i)$, $i \in \mathcal{V}$ is associated to a node in an undirected network structure $\mathcal{G} = (\mathcal{V}, \mathcal{E})$ where an edge $(i, j) \in \mathcal{E}$ represents the ability to exchange information between nodes i and j . This is also represented by the adjacency matrix with entries $\alpha_{i,j} = 1$ if $(i, j) \in \mathcal{E}$, and $\alpha_{i,j} = 0$ otherwise. Unlike divide and conquer approaches (e.g. [1], [2] and [3]), we assume each node periodically shares information on model updates with the nodes in its neighborhood.

In the proposed distributed estimation approach, each node i solves the problem,

$$\min_{\mathbf{w}_i} (f_i(\mathbf{w}_i) + \lambda \rho_i(\mathbf{w}_i)), \quad (4)$$

where

$$f_i(\mathbf{w}_i) = \frac{1}{2} (\mathbf{y}_i - \mathbf{X}_i \mathbf{w}_i)^\top \Omega_i^{-1} (\mathbf{y}_i - \mathbf{X}_i \mathbf{w}_i) \quad (5)$$

is the local measure of model fit, and

$$\rho_i(\mathbf{w}_i) = \frac{1}{2} \sum_{j=1, j \neq i}^N \frac{\alpha_{i,j}}{\text{tr}(\Omega_j)} \|\mathbf{w}_i - \mathbf{w}_j\|^2 \quad (6)$$

is the network regularization penalty, where $\lambda \geq 0$ is a parameter. This differs from the Network Lasso model in [13] is that weights are inversely proportional to the trace of the covariance matrices. If $\lambda = 0$, node i is minimizing local loss in (5). In the other extreme, if $\lambda \rightarrow \infty$, node i is ignoring its own data and opts for a weighted average of neighboring nodes' models.

The localized problem in (4) is equivalent to the global minimization of the following convex loss function,

$$\mathcal{L}_i(\mathbf{w}_1, \dots, \mathbf{w}_N) \triangleq \frac{1}{v} \sum_{i=1}^N \frac{1}{\text{tr}(\Omega_i)} (f_i(\mathbf{w}_i) + \frac{\lambda}{2} \rho_i(\mathbf{w}_i)), \quad (7)$$

where $v = \sum_{i=1}^N 1/\text{tr}(\Omega_i)$ is a normalization constant.

Remark 1. The weight accorded by node i to a neighboring node j in the regularization penalty is akin to the weights used in the optimal combination of forecasts (see [7]). In other words, the penalty associated with disagreement with model j is inversely proportional to the trace of variance-covariance matrix $\text{tr}(\Omega_j)$.

In what follows we shall assume the values of $\text{tr}(\Omega_i)$ are known so that the weights may be readily computed. This assumption is relaxed in Section 4.2 wherein estimates of $\text{tr}(\Omega_i)$ are continuously updated.

2.3 A Distributed Approach with Network Regularization

We consider a network of local learners implementing the following Stochastic Gradient algorithm with a Network regularization penalty (SGN):

$$\mathbf{w}_{i,k+1} = \mathbf{w}_{i,k} - \Gamma(\nabla f_{i,k} + \lambda \nabla \rho_{i,k} + \epsilon_{i,k}), \quad k \in \mathbb{N}^+ \quad (8)$$

where $\nabla f_{i,k}$ and $\nabla \rho_{i,k}$ are the gradient of $f_{i,k}$ and $\rho_{i,k}$ respectively, $\Gamma > 0$ is the step size and $\epsilon_{i,k}$ is the noise introduced by sampling a mini-batch from the given dataset.

We assume $E[\epsilon_{i,k}] = 0$ and $E[\epsilon_{i,k}^2] = \sigma_b^2$. This update assumes node i receives current estimates of its neighbors $\{\mathbf{w}_{j,k}\}_{(i,j) \in \mathcal{E}}$ at each step.

Next, we embed the discrete time process in (8) into a continuous-time domain. Let $\Delta t_{(i,k)}$ be the random time needed by node i to calculate $\nabla f_{i,k}$ and $\nabla \rho_{i,k}$ and complete the update from $\mathbf{w}_{i,k}$ to $\mathbf{w}_{i,k+1}$. We assume that $\Delta t_{(i,k)}$'s are i.i.d. with $E[\Delta t_{(i,k)}] = \Delta t$ and $\mathbf{w}_{i,k}$ is obtained at time $t_{(i,k)} = \sum_{l < k} \Delta t_{(i,l)}$. The process $\{\mathbf{w}_{i,t} : t > 0\}$ is defined as follows:

$$\mathbf{w}_{i,t} \triangleq \mathbf{w}_{i,k}, \quad \text{if } t \in [t_{(i,k)}, t_{(i,k+1)}).$$

Then corresponding continuous expression of (8) is as follows:

$$\mathbf{w}_{i,t_{(i,k+1)}} = \mathbf{w}_{i,t_{(i,k)}} - \Gamma(\nabla f_{i,t_{(i,k+1)}} + \lambda \nabla \rho_{i,t_{(i,k+1)}} + \epsilon_{i,t_{(i,k+1)}}). \quad (9)$$

For notational simplification, we reset $\mathbf{w}_{i,t} := \mathbf{w}_{i,t}/\Gamma$ in the rest of analysis. The continuous time dynamics of $\mathbf{w}_{i,t}$ can be approximated by (see Appendix 5.2):

$$d\mathbf{w}_{i,t} = -\gamma(g_{i,t} + \lambda r_{i,t})dt + \tau_i \gamma \left(\frac{\sigma_b}{\sigma_i} I + \mathbf{X}_i^\top \Omega_i^{-1} \right) dB_{i,t} + \varsigma \gamma \mathbf{X}_i^\top \Omega_i^{-1} \Lambda_i dB_t, \quad (10)$$

where $g_{i,t} := \mathbf{X}_i^\top \Omega_i^{-1} \mathbf{X}_i (\mathbf{w}_{i,t} - \mathbf{w}^*)$ and $r_{i,t} := \sum_{j \neq i} \alpha_{i,j} (\mathbf{w}_{i,t} - \mathbf{w}_{j,t}) / \text{tr}(\Omega_j)$ as per (5) and (6); $\gamma = 1/\Delta t$, $\tau_i = \sigma_i \sqrt{\Gamma \Delta t}$, and $\varsigma = \sqrt{\Gamma \Delta t}$. Here $B_{i,t}$ and B_t are the standard m dimensional Brownian Motion approximating the individual noise associated with node i and the common noise, respectively. In what follows we shall characterize the convergence of the SGN scheme defined in (8) via the continuous-time approximation given in (10).

3 Convergence Analysis

To characterize convergence we will use measures of *consistency* and *regularity*. Let $\hat{\mathbf{w}}_t$ denote the weighted average solution at time t , i.e.,

$$\hat{\mathbf{w}}_t = \frac{1}{v} \sum_{i=1}^N \frac{\mathbf{w}_{i,t}}{\text{tr}(\Omega_i)}. \quad (11)$$

Let $V_{i,t} = \|\mathbf{e}_{i,t}\|^2/2$, where $\mathbf{e}_{i,t} := \mathbf{w}_{i,t} - \hat{\mathbf{w}}_t$. To measure regularity, we will use the weighted average difference between the solutions obtained from a single node and that of the ensemble (weighted) average:

$$\bar{V}_t = \frac{1}{v} \sum_{i=1}^N \frac{\|\mathbf{w}_{i,t} - \hat{\mathbf{w}}_t\|^2}{2\text{tr}(\Omega_i)} = \frac{1}{v} \sum_{i=1}^N \frac{V_{i,t}}{\text{tr}(\Omega_i)}. \quad (12)$$

To measure consistency we will examine the distance between the average and the ground truth,

$$U_t = \frac{1}{2} \|\hat{\mathbf{w}}_t - \mathbf{w}^*\|^2. \quad (13)$$

3.1 Preliminaries

We will make use of the following definitions and results in the convergence analysis.

We define the Laplacian matrix of \mathcal{G} as $L = \hat{\Delta} - A$, where $\hat{\Delta}$ is a diagonal matrix whose i th diagonal entry is equal to the degree of i th node and $A = [\alpha_{i,j}/\text{tr}(\Omega_i)\text{tr}(\Omega_j)]_{i,j}$ is the corresponding adjacency matrix. Let a_2 be the second smallest eigenvalue of L .

The continuous-time gradient $g_{i,t}$ defined above is a function of $\mathbf{w}_{i,t}$, which we do not explicitly specify to simplify notation. In our analyses, we denote $g_{i,t}(\hat{\mathbf{w}}_t) = \mathbf{X}_i^\top \Omega_i^{-1} \mathbf{X}_i (\hat{\mathbf{w}}_t - \mathbf{w}^*)$ and $g_{i,t}(\mathbf{w}^*) = \mathbf{X}_i^\top \Omega_i^{-1} \mathbf{X}_i (\mathbf{w}^* - \mathbf{w}^*)$. Note that $g_{i,t}(\mathbf{w}^*) = 0$ for all $i \in \mathcal{V}$ and t , to simplify notation we will write $g(\mathbf{w}^*)$ instead. Similarly, when a property holds for all t , we drop t and write $g_{i,t}$ as g_i .

We note that g_i 's are μ -Lipschitz continuous and the corresponding loss function (noise-free version of f_i) is strongly convex with κ . To see this, we note that Ω_i^{-1} is positive definite, and can be expressed as $\Omega_i^{-1} = P_i^\top P_i$, where P_i is the matrix resulting from the eigendecomposition. Let $\mathbf{w}_{i,1}$ and $\mathbf{w}_{i,2}$ be two input vectors taken from the function domain, then

$$\begin{aligned} \|g_i(\mathbf{w}_{i,1}) - g_i(\mathbf{w}_{i,2})\| &= \|\mathbf{X}_i^\top \Omega_i^{-1} \mathbf{X}_i (\mathbf{w}_{i,1} - \mathbf{w}_{i,2})\| \\ &\leq \mu \|\mathbf{w}_{i,1} - \mathbf{w}_{i,2}\|, \end{aligned} \quad (14)$$

where $\mu = \max_i \|P_i \mathbf{X}_i\|_F$ and $\|\cdot\|_F$ is the Frobenius norm. Furthermore,

$$\begin{aligned} &(g_i(\mathbf{w}_{i,1}) - g_i(\mathbf{w}_{i,2}))^\top (\mathbf{w}_{i,1} - \mathbf{w}_{i,2}) \\ &= \|P_i \mathbf{X}_i (\mathbf{w}_{i,1} - \mathbf{w}_{i,2})\|^2 \geq \kappa \|\mathbf{w}_{i,1} - \mathbf{w}_{i,2}\|^2, \end{aligned} \quad (15)$$

for some $0 < \kappa < \min_i \|P_i \mathbf{X}_i\|_F^2$. By Definitions (1) and (2), g_i is strongly convex with κ and the corresponding loss function is Lipschitz continuous with constant μ .

3.2 Regularity

The following result establishes that the sum of regularity and consistency measures is equivalent to the weighted sum of the distances between individual solutions $\mathbf{w}_{i,t}$ and the ground truth \mathbf{w}^* .

Lemma 1. *Consider \bar{V}_t in (12) and U_t in (13). We have*

$$\frac{1}{2v} \sum_{i=1}^N \frac{\|\mathbf{w}_{i,t} - \mathbf{w}^*\|^2}{\text{tr}(\Omega_i)} = \bar{V}_t + U_t. \quad (16)$$

Proof. Proof of Lemma 1. We expand the sum on the left-hand side of (16) as follows,

$$\frac{1}{2v} \sum_{i=1}^N \frac{\|\mathbf{w}_{i,t} - \mathbf{w}^*\|^2}{\text{tr}(\Omega_i)} = \frac{1}{2v} \sum_{i=1}^N \frac{1}{\text{tr}(\Omega_i)} \left[\|\mathbf{w}_{i,t} - \hat{\mathbf{w}}_t\|^2 + \|\hat{\mathbf{w}}_t - \mathbf{w}^*\|^2 + 2\langle \mathbf{e}_{i,t}, \hat{\mathbf{w}}_t - \mathbf{w}^* \rangle \right] \quad (17)$$

where $\mathbf{e}_{i,t} = \mathbf{w}_{i,t} - \hat{\mathbf{w}}_t$. Note that

$$\frac{1}{v} \sum_{i=1}^N \frac{\mathbf{e}_{i,t}}{\text{tr}(\Omega_i)} = \frac{1}{v} \sum_{i=1}^N \frac{\mathbf{w}_{i,t}}{\text{tr}(\Omega_i)} - \hat{\mathbf{w}}_t = 0. \quad (18)$$

Hence, (16) follows by observing that the summation of the cross-product (last) term inside the brackets in (17) is zero. \square

In what follows, we obtain upper bounds on the expectations of regularity \bar{V}_t and consistency U_t processes in Theorems 1 and 2, respectively. Given the relation in Lemma 1, these bounds provide a bound on the average error of individual estimates generated by the SGN algorithm with respect to the ground truth.

The following result provides an upper bound on the expected regularity of the estimates at a given time.

Theorem 1. *Let $\mathbf{w}_{i,t}$ evolve according to continuous time dynamics (10). Then*

$$\mathbb{E}[\bar{V}_t] \leq e^{-2(\kappa + \lambda a_2)\gamma t} \bar{V}_0 + \frac{\gamma C_1}{2(\kappa + \lambda a_2)} (1 - e^{-2(\kappa + \lambda a_2)\gamma t})$$

where C_1 is a constant term given in (34) that depends on the data \mathbf{X} , matrices $\{\Lambda_i\}_{i \in \mathcal{V}}$ and noise variances $\{\sigma_i^2\}_{i \in \mathcal{V}}$. In the long run,

$$\lim_{t \rightarrow \infty} \mathbb{E}[\bar{V}_t] \leq \frac{\gamma C_1}{2(\kappa + \lambda a_2)}.$$

Proof. Proof of Theorem 1. See Appendix 5.3. \square

It is not surprising that the expected difference in estimates decreases with growing λ which penalizes disagreement with neighbors. Similarly, the larger the algebraic connectivity of the network a_2 or the strong convexity constant κ is, the smaller is the expected \bar{V}_t .

Finally, the constant term C_1 (defined in (34)-(35) for exposition purposes) is determined by data \mathbf{X} and the matrices Λ_i . In particular, C_1 is small when we have nodes that are less affected by the noise. Intuitively, with increasing network size, nodes with less exposure to noise are given increasing weight which then increases regularity across estimates. We will make use of this intuition in Lemma 2 to show convergence of weighted average estimate $\hat{\mathbf{w}}_t$ to the ground truth \mathbf{w}^* .

3.3 Consistency

The consistency measure $\{U_t, t \geq 0\}$ captures the performance of the average solution $\hat{\mathbf{w}}$. In the following theorem, we provide a characterization of the performance of the collective effort.

Theorem 2. *Let $\mathbf{w}_{i,t}$ evolve according to continuous time dynamics (10). Then*

$$\mathbb{E}[U_t] \leq e^{-2\kappa\gamma t} U_0 + \frac{\gamma}{2\kappa} \left(\frac{\mu - \kappa}{\lambda a_2} C_1 + C_2 \right) (1 - e^{-2\kappa\gamma t}),$$

where C_1 is defined in (34) and

$$C_2 = \frac{1}{2v^2} \left(\sum_{k=1}^N \frac{\tau_k^2}{\text{tr}(\Omega_k)^2} \|\mathbf{X}_k \Omega_k^{-1}\|_F^2 + \varsigma^2 \sum_{k=1}^N \sum_{j=1}^N \frac{1}{\text{tr}(\Omega_k) \text{tr}(\Omega_j)} \mathbf{1}^\top (\mathbf{X}_k^\top \Omega_k^{-1} \Lambda_k \circ \mathbf{X}_j^\top \Omega_j^{-1} \Lambda_j) \mathbf{1} \right) \quad (19)$$

with “ \circ ” denoting the Hadamard product. In the long run,

$$\lim_{t \rightarrow \infty} \mathbb{E}[U_t] \leq \frac{\gamma}{2\kappa} \left(\frac{\mu - \kappa}{\lambda a_2} C_1 + C_2 \right). \quad (20)$$

Proof. Proof of Theorem 2. See Appendix 5.4. \square

Similar to the regularity measure bound, the penalty constant λ and the algebraic connectivity a_2 reduce the bound on the expected consistency. However, the long run expected difference between collective estimate and ground truth does not reduce to zero as $\lambda a_2 \rightarrow \infty$. Indeed, we cannot expect the collective performance to improve above a given level by increasing connectivity or increasing regularity among different models. The constant C_2 , determined by the data \mathbf{X} and matrices Λ_i , captures the performance gap in the long run due to available data. We can only improve performance by addition of new nodes that have access to more reliable data.

We state the convergence to the optimal solution in the case of growing network size in the following lemma.

Lemma 2. (Consistency) *Assume the network of local learners (with associated data sets) grows as follows:*

- Each new node (say $n > N$, $N = 1, 2, \dots$) is associated with a new dataset $(\mathbf{X}_n, \mathbf{y}_n)$ given by (1) with

$$\|X_n\|_F < L_0, \quad \text{tr}(\Omega_n) \leq M, \quad \text{and } \epsilon \leq \sigma_n^2,$$

where $L_0 < \infty$, and $0 < \epsilon < M < \infty$.

- The network connectivity is preserved.

If we have $\lambda a_2 \sim N$, and $\Gamma \sim \epsilon^4$, then

$$\lim_{t \rightarrow \infty} \lim_{N \rightarrow \infty} \mathbb{E}[\|\hat{\mathbf{w}}_t - \mathbf{w}^*\|^2] = \lim_{t \rightarrow \infty} \lim_{N \rightarrow \infty} \mathbb{E}[U_t] < \frac{S_2 M^2 \Gamma}{2m\kappa\epsilon^3} = O(\Gamma^{1/4}),$$

where $S_2 = \max_{k,j} \max_i \mathbf{x}_{i,k}^\top \mathbf{x}_{i,j}$ with $\mathbf{x}_{i,k}$ being the k -th column of \mathbf{X}_i^\top .

Proof. Proof of Lemma 2. See Appendix 5.5. \square

The proof follows by constructing an upper bound for (20) in Theorem 2 by considering constants C_1 and C_2 . We first show that all terms of C_2 can be bounded by $S_2 M^2 \Gamma \Delta t / (m \epsilon^3)$ by using the assumptions on each new dataset available to each new node. This bound on C_2 increases with the noise term that affects the nodes, the magnitude of the inputs, Δt and step size, and decreases with the size of the dataset available to each node and the strong convexity term. Second, show that C_1/N goes to zero as $N \rightarrow \infty$. Combining the limiting properties of the two constants with the bound in (20) and selecting λ such that $\lambda a_2 \sim N$, we obtain the bound above. This bound can be controlled by selection of the step size Γ . Note that we can make $\lambda a_2 \sim N$ by adjusting the penalty parameter when the network retains connectivity as the number of nodes grows.

Remark 2. Lemma 2 provides an upper bound of the difference between the ensemble average estimate and the ground truth, which is $O(\Gamma^{1/4})$ as $N \rightarrow \infty$. The bound is subject to the influence of the data: less noisy (smaller $\text{tr}(\Omega_i)$), and smaller in magnitude (smaller S_2) leads to a tighter bound. We observe that the bound is tighter when the object function is smoother (larger κ) and the nodes receive more data points (larger m). Since we require $\Gamma \sim \epsilon^4$ (or even smaller Γ), the effect of having small ϵ is offset by choosing smaller Γ . Thus the bound can be controlled as small as needed by choosing the stepsize Γ .

3.4 Comparison with Centralized Estimation

In the centralized model, the observation vector \mathbf{y} in (3) can be expressed in (2). Let $B_{c_1,t}$ and $B_{c_2,t}$ be standard p dimensional Brownian Motions that approximating ε and ξ respectively. Suppose we utilize the SGD method to solve (3), similar to the analysis of (10), the corresponding stochastic differential equation is

$$d\mathbf{w}_t = -g_t \gamma dt + \tau \gamma D \mathbf{X}^\top \Omega^{-1} dB_{c_1,t} + \varsigma \gamma \mathbf{X}^\top \Omega^{-1} \Lambda dB_{c_2,t}, \quad (21)$$

where $g_t = \mathbf{X}^\top \Omega^{-1} \mathbf{X}(\mathbf{w}_t - \mathbf{w}^*)$, $\tau = \sqrt{\Gamma \Delta t}$, and D is a block diagonal matrix with i -th block equal to $\sigma_i I_m$. We define the measure

$$G_t = \frac{1}{2} \|\mathbf{w}_t - \mathbf{w}^*\|^2,$$

and it follows that

$$dG_t = -\gamma g_t^\top (\mathbf{w}_t - \mathbf{w}^*) dt + K_3 d\tilde{B}_{c,t} + \gamma^2 C_3 dt,$$

where $K_3 d\tilde{B}_{c,t}$ is the summation of the Ito terms, and C_3 is the summation of the constant terms:

$$K_3 d\tilde{B}_{c,t} = \tau \gamma (\mathbf{w}_t - \mathbf{w}^*)^\top D \mathbf{X}^\top \Omega^{-1} dB_{c_1,t} + \varsigma \gamma (\mathbf{w}_t - \mathbf{w}^*)^\top \mathbf{X}^\top \Omega^{-1} \Lambda dB_{c_2,t}$$

$$C_3 = \frac{1}{2} (\tau^2 \|D \mathbf{X}^\top \Omega^{-1}\|_F^2 + \varsigma^2 \|\mathbf{X}^\top \Omega^{-1} \Lambda\|_F^2).$$

Similar to the analysis of Theorem 2, we can obtain

$$dG_t \leq -2\kappa_1 \gamma G_t dt + C_3 \gamma^2 dt + K_3 d\tilde{B}_{c,t},$$

with $0 < \kappa_1 < \|\mathbf{X} \Omega^{-1}\|_F^2$, it follows that

$$\mathbb{E}[G_t] \leq e^{-2\kappa_1 \gamma t} G_0 + \frac{\gamma}{2\kappa_1} C_3 (1 - e^{-2\kappa_1 \gamma t}). \quad (22)$$

In the long run,

$$\mathbb{E}[G_t] \leq \frac{\gamma}{2\kappa_1} C_3.$$

Remark 3. We would like to compare the long run performance of the SGN scheme and that of centralized estimation. When choosing λ such that $\lambda a_2 \sim N$, the problem reduces to comparing C_3/κ_1 and C_2/κ . We can consider the two terms of C_2 in (19) as weighted average of that of C_3 . On the one hand, the distributed approach gives more weight to the nodes that are subject to less common noise, which has noise reduction effect. With proper choice of N , C_2 can be smaller than C_3 . On the other hand, determined by the data, κ_1 is generally greater than κ . In summary, if the number of nodes (N) increases, the performance of the distributed algorithm can be close to that of the centralized algorithm.

4 Numerical Illustrations

In this section, we will apply the proposed method to three examples to corroborate analytical results. First, we apply the SGN algorithm to a MRF estimation problem using a WSN with synthetic data. Next, we look at a real-world problem: the escape behavior of European gregarious birds and compare our scheme with a centralized estimator computed by solving the generalized least squares (GLS). Finally, we consider a synthetic dataset to analyze the effects of number of nodes, network structure and the regularization penalty parameter.

4.1 Temperature Estimation of a Field

We consider a WSN deployed to estimate the temperature on a $20\text{m} \times 20\text{m}$ field, which is divided into 400 equal squares. We assume that the temperature within the same square is the same, and the true temperature of the field is stored in the vector $\mathbf{w}^* \in \mathbb{R}^{400 \times 1}$. We randomly place N sensors on the field and each measures \mathbf{w}^* using noisy local observations $\mathbf{y}_i \in \mathbb{R}^{400 \times 1}$, which is corrupted by the measurement noise ε_i , a detection error that only influence sensor i ; and the network disturbance ξ , a common noise that is shared by all sensors. Each sensor i only shares a portion of ξ , which is determined by a matrix Λ_i . Λ_i values reflect the relative distance between the locations of the sensor and the measured squares: a sensor that is close to a square is subject to lower noise levels. We assume \mathbf{w}^* is fixed but \mathbf{y}_i changes at each measurement, which can be expressed as follows:

$$\mathbf{y}_i = \mathbf{w}^* + \varepsilon_i + \Lambda_i \xi, \quad (23)$$

where $\varepsilon_i \sim \mathcal{N}_m(\mathbf{0}, \sigma^2 \mathbf{I})$ and $\xi \sim \mathcal{N}_m(\mathbf{0}, \mathbf{I})$. Note that if we set $\mathbf{X}_i = \mathbf{I}$, (1) and (23) have the same form.

We model the temperature of the field using a Gaussian MRF and let the temperature values range from 0°F to 255°F , as in [22]. Two heat locations are located at $(5m, 17m)$ and $(17m, 19m)$, and temperature drops from the heat source at a rate of 25°F/m within an area of influence of 3m from the source. We set $N = 200$ and randomly connect the nodes to their neighbors within 2m—see Figure 1(a) for sensor locations and heat map of the field.

Each node has the following local cost,

$$\mathcal{L}(\mathbf{w}_i) = (\mathbf{y}_i - \mathbf{w}_i)^\top \Omega_i^{-1} (\mathbf{y}_i - \mathbf{w}_i) + \frac{1}{2} \sum_{j \in \mathcal{V} \setminus i} \frac{\alpha_{i,j}}{\lambda_j} \|\mathbf{w}_i - \mathbf{w}_j\|^2 \quad (24)$$

where λ_i is a constant that represents the smoothness of the changes in the temperature. In this experiment, we set $\lambda_j = \text{tr}(\Omega_i)/\lambda$ for each i . By doing so, (24) has the same form as (4).

We would like to minimize the cost function (24) for each sensor by selecting proper \mathbf{w}_i . We set the stepsize $\Gamma = 0.01$ and the penalty parameter $\lambda = 100$ for SGN. Figure 1(b) shows the

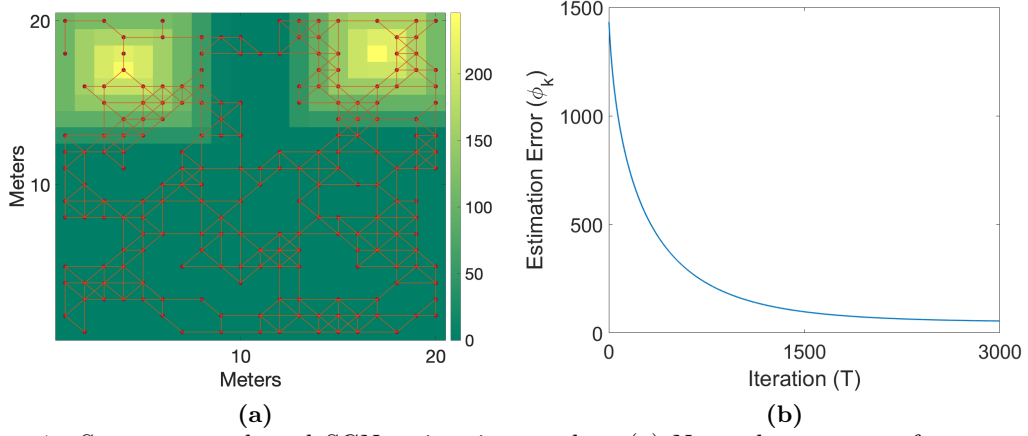


Figure 1. Sensor network and SGN estimation results. (a) Network structure of sensors. The orange dots denote the nodes, and the lines denote the edges between nodes. The two heat sources are located at $(5m, 17m)$ and $(17m, 19m)$, marked by yellow. (b) SGN estimation error ϕ_k at each iteration. The final estimation error $\phi_T = 55$.

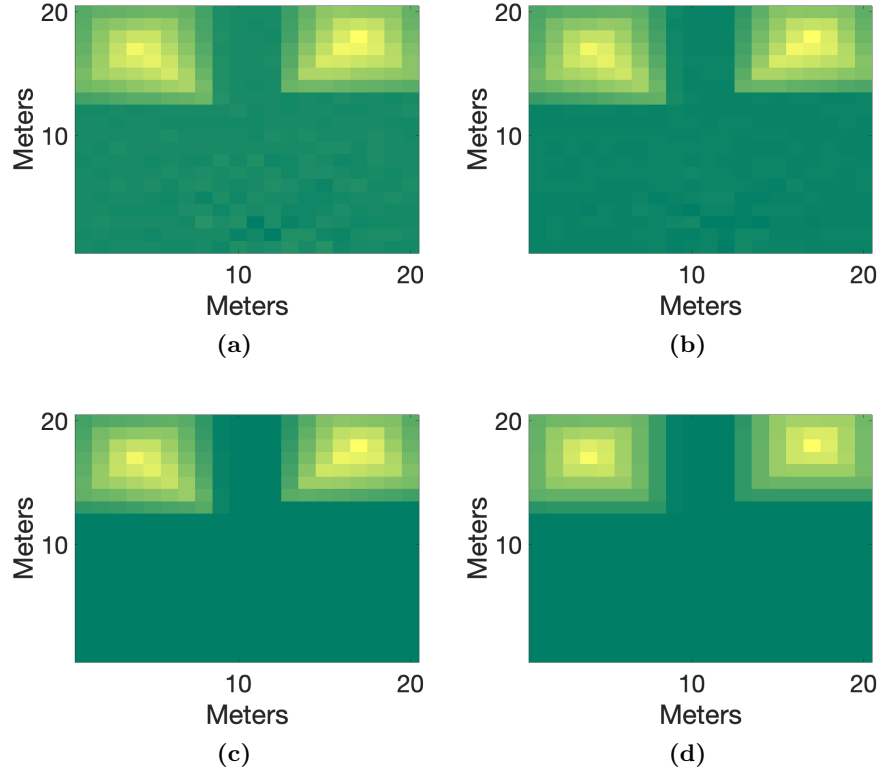


Figure 2. Field temperature estimation from a single node (the 150-th sensor at $(10m, 7m)$). (a)-(d) display the sensor estimations at time points $t = 4$, $t = 10$, $t = 100$, and $t = 2000$, respectively.

decrease of the estimation error $\phi_k = \|\hat{\mathbf{w}}_k - \mathbf{w}^*\|$ over the iterations of SGN. Figure 2 presents the estimations of a single node (the 150th sensor at location (10m, 7m)). The estimates are noisy at the early stage ($t = 4$). By time $t = 10$, we observe significant noise reduction compared to the first few iterations. This reduction becomes more substantial at $t = 100$. At $t = 2000$, the temperature estimations of 150th sensor are very close to the true temperature values.

4.2 Unknown Variance-Covariance

Next, we apply our scheme to a real-world problem where we investigate the influencing factors of the birds escape behavior. [23] uses the Flight initiation distance (FID), the distance at which animals take flight from approaching threats, to study the predator-prey interactions and prey escape behavior. In this example, the FID is considered as the response variable, and the predictors are flock size (the number of aggregated individuals of the same species), starting distance ((start dist) the distance at which a predator started the approach to the bird), habitat type (binary with urban= 1 and rural= 0), latitude (of the study location), diet (primary type of food the bird consumed, all species were classified into 5 main categories: granivorous(g), granivorous-insectivorous(gi), insectivorous(i), carnivorous(c), and carrion-eater(ca)) [24]. We transform the variable “diet” into 5 binary variables, each indicating one diet category, and normalize all other variables for the following analysis. At each node, the FID estimate is given by

$$\widehat{FID} = w_0 + w_1 \cdot \text{start dist} + w_2 \cdot \text{diet(gi)} + w_3 \cdot \text{diet(g)} + w_4 \cdot \text{diet(i)} + w_5 \cdot \text{latitude} + w_6 \cdot \text{flock} + w_7 \cdot \text{habitat},$$

where we denote node i ’s estimate with $\mathbf{w}_i = [w_0, \dots, w_7]$ as before. The data contains 941 observations in total collected from eight European countries. The data contains 23 different bird species.

We group 23 bird species into $N = 15$ nodes where each species is assigned only to a single node. Each node contains more than 10 observations, and nodes do not necessarily have the same number of observations. We construct the random network as a N -node complete network—see Figure 3(a). We use the mini-batch process in this example and set the mini-batch sample size as 10. The covariance matrix of a node is computed as the diagonals of the covariance matrix of 15 mini-batch samples. We use a fading memory update rule to compute the trace of the covariance matrix, $\text{tr}(\Omega_i)$, [25]:

$$\text{tr}(\Omega_{i,k+1}) = \varphi \text{tr}(\Omega_{i,k}) + (1 - \varphi) \text{tr}(\hat{\Omega}_{i,k+1}),$$

where $\text{tr}(\hat{\Omega}_{i,k+1})$ is the i -th covariance matrix trace computed at the $k + 1$ -th iteration, and $\varphi \in (0, 1)$ is the fading parameter that controls the memory of the past covariance values. For SGN experiments in this section, we set parameter $\varphi = 0.9$, the step size $\Gamma = 0.001$, and the regularization penalty $\lambda = 100$.

The estimation error at step k of SGN is given by $\phi_k = \|FID - \mathbf{X}\hat{\mathbf{w}}_k\|$, where \mathbf{X} is the matrix containing the observations and $\hat{\mathbf{w}}_k$ is the weighted estimation (11) from SGN. We define average estimation error $\bar{\phi}_k$ as the average of estimation errors at step k (ϕ_k) over 20 runs. Figure 3(b) shows that the average estimation error $\bar{\phi}_k$ of SGN converges after 2000 iterations. We compare the final estimator $\hat{\mathbf{w}}_T$ after $T = 3000$ iterations of SGN with the solution of the GLS in Table 1. Half of the SGN estimators fall into the 97% confidence interval of the GLS estimators. The average estimation error of SGN at the final step ($\bar{\phi}_T = 20.45$) is close to the estimation error of GLS (19.31). Figure 3(c) shows the difference between the estimates from both methods (using estimators in Table 1) relative to the ground truth. The difference in estimates is small for majority of the observations.

Regressor	GLS	SGN	CI(GLS)	
Intercept	0.5614	0.2204	[0.4267, 0.6962]	
Start dist	0.372	0.1958	[0.3132, 0.4308]	
Diet(gi)	-0.474	-0.3397	[-0.6128, -0.3352]	*
Diet(g)	-0.2781	-0.0670	[-0.4542, -0.1021]	
Diet(i)	-0.4715	-0.2993	[-0.6448, -0.2981]	*
Latitude	-0.0946	-0.0548	[-0.1425, -0.0467]	*
Flock	-0.4886	-0.3377	[-0.5796, -0.3976]	
Habitat	0.0463	0.0280	[0.0009, 0.0917]	*

Table 1. Results of GLS and SGN estimations, accounting for variation in FID in relation to starting distance, diet, latitude, flock size, habitat in European gregarious bird species. CI(GLS) is the 97% confidence interval of the GLS estimations and the SGN estimations are marked by * if they fall into CI(GLS).

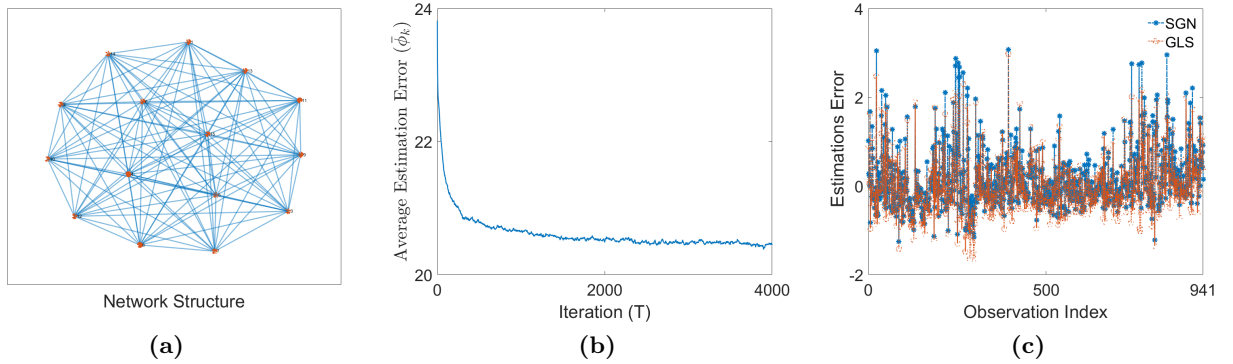


Figure 3. GLS and SGN estimation results. (a) Network structure of birds escape problem using SGN. The orange dots denote the nodes, and the blue lines denote the edges between the nodes. (b) SGN average estimation error $\bar{\phi}_k$ at each iterations. (c) Difference between true FID and the estimations from GLS and SGN (\widehat{FID}) for each observation.

4.3 Effects of Network Connectivity and regularization

We consider a synthetically generated dataset that satisfies the assumptions of the setup in Section 2.1 in order to test the effects of (a) growing network size N , (b) network connectivity and (c) regularization penalty λ .

The numerical setup that is common to all experiments in this section is as follows. Each node receives 10 data points ($m = 10$), and there are 5 features ($d = 5$), i.e., $\mathbf{X}_i \in \mathbb{R}^{10 \times 5}$. We generate feature values \mathbf{X}_i randomly using a normal distribution with mean 1 and variance 0.1^2 . The individual noise term for each node comes from a zero-mean normal distribution with variance σ_i^2 randomly chosen between 0.001^2 - 0.1^2 . The matrix Λ_i is randomly created with its norm controlled between 0.003-0.3 for all $i \in \mathcal{V}$. The output y_i 's are generated according to (1) with \mathbf{w}^* set as a vector of random integers. For all the experiments, SGN stepsize is $\Gamma = 10^{-8}$ and the total number of iterations is set to $T = 1000$.

In the first experiment, we look at the effect of network size. With each new node added we increase the data size by m , i.e., $p = Nm$, while keeping $\lambda = 100$ fixed. Given an N value, we run SGN for 10 trials. For each trial, we generate a random network with N nodes by randomly keeping $\Upsilon_N = 0.6$ fraction of the edges from the complete N -node network. We measure the performance given N nodes using scaled final average estimation error $\Phi_s(N)$ in Figure 4(a). We compute $\Phi_s(N)$ by averaging final estimation errors ϕ_{1000} of 10 trials ($\bar{\phi}_T(N, \lambda = 100)$) and then dividing it by the average final estimation error when $N = 5$ and $\lambda = 0$, $\bar{\phi}_T(N = 5, \lambda = 0)$. The scaling term $\bar{\phi}_T(N = 5, \lambda = 0)$ makes sure $\Phi_s(N) \in (0, 1)$ for all $N \in [5, 150]$. Figure 4(a) shows a decrease of 15% in average estimation error when we increase N from 5 to 150 while keeping regularization penalty and connectivity the same.

In the second experiment, we fix $N = 100$ and $\lambda = 100$ while ranging Υ_{100} from 0 to 1. We recall Υ_{100} determines the fraction of edges kept from the complete 100-node network. In Figure 4(b), the average estimation error is scaled with $\bar{\phi}_T(N = 100, \lambda = 0)$ and computed over 10 trials for a given Υ_{100} . Note that the case when $\Upsilon_{100} = 0$, i.e., when the network is fully disconnected, is equivalent to having $\lambda = 0$. Here we observe that addition of new edges improves the performance of SGN when N is fixed. Indeed, the expected decrease in estimation error is about 20% when we compare the fully disconnected case with the complete network.

In the third experiment, we fix the number of nodes $N = 20$, and the network connectivity $\Upsilon_N = 0.6$, while varying the regularization penalty λ . We compute scaled average estimation error Φ_s similarly as before using 10 trials and $\bar{\phi}_T(N = 20, \lambda = 0)$ as the base average estimation value. In Figure 4(c), we report the average estimation error with respect to penalty scale $\iota \in [0, 1)$ where $\lambda = \iota/(1 - \iota)$. That is, a larger λ means a larger ι —see figure caption for details. We observe that as the regularization penalty is increased from the value of 99 to 9999, the performance improves.

Overall, the numerical experiments in this section support the consistency bound in Theorem 2 and the convergence to optimality in Lemma 2 for the SGN method.

5 Conclusions

The ever-increasing dimension of data and the size of datasets have introduced new challenges to centralized estimation. For example, limited bandwidth in current networking infrastructure may not satisfy the demands for transmitting high-volume datasets to a central location. Hence, it is of interest to study alternatives to centralized estimation.

In this paper we consider a distributed architecture for learning a linear model via generalized least squares by relying on a network of interconnected “local” learners. In the proposed distributed scheme, each computer (or local learner) is assigned a dataset and *asynchronously* im-

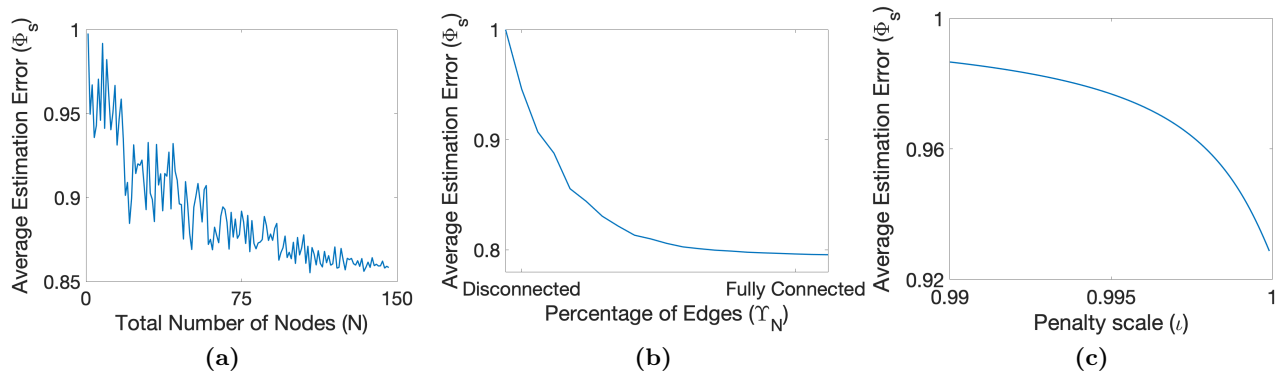


Figure 4. Node size, connectivity and regularization parameter effects. (a) Average estimation error Φ_s as N and p increases. (b) Average estimation error Φ_s as the fraction of edges Υ_N increases. The network is disconnected when $\Upsilon_N = 0$, and is fully connected when $\Upsilon_N = 1$. (c) Average estimation error Φ_s as the regularization penalty λ increases. We observe slow decrease of Φ_s from 1 to 0.98 when ι ranging from 0 to 0.99 (or λ from 0 to 99 equivalently). Here we only present the range of $\iota \in [0.99, 0.9999]$, i.e., range when $\lambda \in [99, 9999]$.

plements stochastic gradient updates based upon a sample (or a mini-batch) sample. To ensure robust estimation, a network regularization term which penalizes models with high *local* variability is used. Unlike other model averaging schemes based upon a synchronized step, the proposed scheme implements local model averaging continuously and asynchronously. We provide finite-time performance guarantees on consistency. We illustrate the application of the proposed method for estimation in a Markov Random Field with synthetic datasets and a real dataset from ecology.

Appendix

5.1 Technical preliminaries

We will make use of the following definitions and Ito's lemma. Let $f : \mathcal{X} \rightarrow \mathcal{S}$ be a function with gradient $\nabla f(x)$.

Definition 1. f is called a Lipschitz function if there exists a constant $\mu > 0$, such that

$$\|f(x_1) - f(x_2)\| \leq \mu \|x_1 - x_2\|$$

for some all $x_1, x_2 \in \mathcal{X}$.

Definition 2. f is said to be strictly convex, if

$$(\nabla f(x_1) - \nabla f(x_2))^T (x_1 - x_2) \geq \kappa \|x_1 - x_2\|^2$$

for some $\kappa > 0$ and all $x_1, x_2 \in \mathcal{X}$.

Lemma 3. Multidimensional Ito Lemma [26]

Let

$$dX_t = \mathbf{u}dt + VdB_t$$

be an m -dimensional Ito process, where \mathbf{u} is a vector of length m , V is an $m \times m$ matrix, and B_t is a m -dimensional Brownian motions. Let $g_{t,x}$ be a twice differentiable map from \mathbb{R}^m into \mathbb{R} . Then the process

$$Y_t = g_{t,X_t}$$

is again an Ito process with

$$dY_t = \frac{\partial g}{\partial t} dt + \sum_i \frac{\partial g}{\partial x_i} dX_i + \frac{1}{2} \sum_{i,j} \frac{\partial^2 g}{\partial x_i \partial x_j} dX_i dX_j,$$

where $dX_i dX_j$ is computed using rules $dt dt = 0$, $dt dB_i = 0$, $(dB_i)^2 = mdt$, $B_{i,t} B_t = 0$, and $B_i B_j = 0$ for all $i \neq j$.

5.2 Continuous Time Representation of the Approximation Dynamics

In this section, we will derive the formula of $d\mathbf{w}_{i,t}$ by rewriting the scheme (9) in the form of the summation of previous steps, and approximate the noise terms by standard m -dimensional Brownian motions and the rest by integrals. Then $d\mathbf{w}_{i,t}$ can be approximated by the differential form of a stochastic Ito integral. We initially assume both noise terms have zero-mean Gaussian distribution: $\xi \sim \mathcal{N}_m(\mathbf{0}, \mathbf{I}_m)$ and $\varepsilon_i \sim \mathcal{N}_m(\mathbf{0}, \sigma_i^2 \mathbf{I}_m)$ for all i . Later we show via Central Limit Theorem that this approximation also holds for general distributions.

5.2.1 Approximation with Gaussian distributed noise term

For each node $i \in \mathcal{V}$, we trace back to the initial step from the current iteration, and rewrite the scheme (9) in the form of summation of all previous iterations:

$$\begin{aligned} \mathbf{w}_{i,t} = & \mathbf{w}_{i,0} - \Gamma \sum_{\Gamma l < t} \left[\mathbf{X}_i^T \Omega_i^{-1} \mathbf{X}_i (\mathbf{w}_{i,\Gamma t(i,l)} - \mathbf{w}^*) + \lambda \sum_{j=1, j \neq i}^N \frac{\alpha_{i,j}}{\text{tr}(\Omega_j)} (\mathbf{w}_{i,\Gamma t(i,l)} - \mathbf{w}_{j,\Gamma t(i,l)}) \right] \\ & + \Gamma \mathbf{X}_i^T \Omega_i^{-1} \sum_{\Gamma l < t} \varepsilon_{i,l} + \Gamma \mathbf{X}_i^T \Omega_i^{-1} \Lambda_i \sum_{\Gamma l < t} \xi_l + \Gamma \sum_{\Gamma l < t} \epsilon_l, \end{aligned} \quad (25)$$

Let n_t be the number of the updates completed up to time t , i.e., $n_t := |\{l \in \mathbb{N} : \Gamma t_{(i,l)} < t\}|$. Recall that we assume $\Delta t_{(i,k)}$'s are i.i.d. with $\mathbb{E}[\Delta t_{(i,k)}] = \Delta t$ and $\mathbf{w}_{i,k}$ is obtained at time $t_{(i,k)} = \sum_{l < k} \Delta t_{(i,l)}$. By strong law of large numbers, for small Γ ,

$$\frac{\Gamma n_t}{t} \simeq \frac{1}{\Delta t}. \quad (26)$$

Consider the second term in (25). Let $\gamma = 1/\Delta t$, we approximate the discrete processes by integrals using (26):

$$\begin{aligned} \Gamma \sum_{\Gamma l < t} \mathbf{X}_i^\top \Omega_i^{-1} \mathbf{X}_i (\mathbf{w}_{i,\Gamma t(i,l)} - \mathbf{w}^*) &= \frac{\Gamma n_t}{t} \sum_{\Gamma l < t} \mathbf{X}_i^\top \Omega_i^{-1} \mathbf{X}_i (\mathbf{w}_{i,\Gamma t(i,l)} - \mathbf{w}^*) \frac{t}{n_t} \\ &= \gamma \int_0^t \mathbf{X}_i^\top \Omega_i^{-1} \mathbf{X}_i (\mathbf{w}_{i,s} - \mathbf{w}^*) ds, \text{ and} \end{aligned} \quad (27)$$

$$\begin{aligned} \lambda \Gamma \sum_{\Gamma l < t} \sum_{j=1, j \neq i}^N \frac{\alpha_{i,j}}{\text{tr}(\Omega_j)} (\mathbf{w}_{i,\Gamma t(i,l)} - \mathbf{w}_{j,\Gamma t(i,l)}) &= \lambda \frac{\Gamma n_t}{t} \sum_{\Gamma l < t} \sum_{j=1, j \neq i}^N \frac{\alpha_{i,j}}{\text{tr}(\Omega_j)} (\mathbf{w}_{i,\Gamma t(i,l)} - \mathbf{w}_{j,\Gamma t(i,l)}) \frac{t}{n_t} \\ &= \lambda \gamma \int_0^t \sum_{j=1, j \neq i}^N \frac{\alpha_{i,j}}{\text{tr}(\Omega_j)} (\mathbf{w}_{i,s} - \mathbf{w}_{j,s}) ds. \end{aligned} \quad (28)$$

Now consider the individual noise. Since we assume $\varepsilon_i \sim \mathcal{N}_m(\mathbf{0}, \sigma_i^2 \mathbf{I})$, all components of ε_i are independent and it is enough to illustrate one-dimension approximation. Let $\varepsilon_{i,l}^{(q)}$ be the q th dimension of $\varepsilon_{i,l}$, and for all $q \in \mathcal{D} = \{1, \dots, m\}$, it follows that

$$\mathbb{E}[\Gamma \sum_{\Gamma l < t} \varepsilon_{i,l}^{(q)}] = 0, \text{ and}$$

$$\text{Var}[\Gamma \sum_{\Gamma l < t} \varepsilon_{i,l}^{(q)}] = n_t \Gamma^2 \sigma_i^2 = \frac{\Gamma n_t}{t} t \Gamma \sigma_i^2 = \gamma \Gamma \sigma_i^2 t.$$

We approximate $\sum_{\Gamma l < t} \varepsilon_{i,l}$ by a standard m -dimensional Brownian Motion $B_{i,t}$:

$$\Gamma \sum_{\Gamma l < t} \varepsilon_{i,l} \approx \sigma_i \sqrt{\Gamma \frac{1}{\gamma}} \gamma B_{i,t} = \tau_i \gamma B_{i,t},$$

where $\tau_i = \sigma_i \sqrt{\Gamma \Delta t}$. Hence the individual noise term in (25) can be approximated as

$$\Gamma \mathbf{X}_i^\top \Omega_i^{-1} \sum_{\Gamma l < t} \varepsilon_{i,l} \approx \tau_i \gamma \mathbf{X}_i^\top \Omega_i^{-1} B_{i,t}. \quad (29)$$

Similar to the proof of the individual noise approximation, let $\xi_{i,l}^{(q)}$ be the q th dimension of $\xi_{i,l}$, for $q \in \mathcal{D}$, the it follows that

$$\mathbb{E}[\Gamma \sum_{\Gamma l < t} \xi_{i,l}^{(q)}] = 0, \text{ and}$$

$$\text{Var}[\Gamma \sum_{\Gamma l < t} \xi_{i,l}^{(q)}] = \frac{\Gamma n_t}{t} t \Gamma = \gamma \Gamma t.$$

Let $\varsigma = \sqrt{\Gamma\Delta t}$, then we approximate the common noise term in (25) by a standard m -dimensional Brownian Motion B_t :

$$\Gamma \mathbf{X}_i^\top \Omega_i^{-1} \Lambda_i \sum_{\Gamma l < t} \xi_l \approx \varsigma \gamma \mathbf{X}_i \Omega_i^{-1} \Lambda_i B_t. \quad (30)$$

Let $\epsilon_{i,l}^{(q)}$ be the q th dimension of $\epsilon_{i,l}$, then for all $q \in \mathcal{D}$, then

$$\begin{aligned} \mathbb{E}\left[\Gamma \sum_{\Gamma l < t} \epsilon_{i,l}^{(q)}\right] &= 0, \text{ and} \\ \text{Var}\left[\Gamma \sum_{\Gamma l < t} \epsilon_{i,l}^{(q)}\right] &= \frac{\Gamma n_t}{t} t \Gamma \sigma_b^2 = \gamma \Gamma \sigma_b^2 t. \end{aligned}$$

Similar to (29), we can approximate the gradient error in (25) by $B_{i,t}$,

$$\Gamma \sum_{\Gamma l < t} \epsilon_{i,l} \approx \sigma_b \sqrt{\Gamma \frac{1}{\gamma}} \gamma B_{i,t} = \sigma_b \sqrt{\Gamma \Delta t} \gamma B_{i,t}. \quad (31)$$

Combining (29) and (31), the Brownian term $B_{i,t}$ becomes

$$\sigma_b \sqrt{\Gamma \Delta t} \gamma B_{i,t} + \sigma_i \sqrt{\Gamma \Delta t} \gamma \mathbf{X}_i^\top \Omega_i^{-1} B_{i,t} = \tau_i \gamma \left(\frac{\sigma_b}{\sigma_i} I + \mathbf{X}_i^\top \Omega_i^{-1} \right) B_{i,t}. \quad (32)$$

Substituting (27), (28), (30), and (32) to the corresponding terms in (25), $\mathbf{w}_{i,t}$ approximately satisfies the following stochastic Ito integral:

$$\begin{aligned} \mathbf{w}_{i,t} = & \mathbf{w}_{i,0} - \gamma \int_0^t \mathbf{X}_i^\top \Omega_i^{-1} \mathbf{X}_i (\mathbf{w}_{i,s} - \mathbf{w}^*) ds - \lambda \gamma \int_0^t \sum_{j=1, j \neq i}^N \frac{\alpha_{i,j}}{\text{tr}(\Omega_j)} (\mathbf{w}_{i,s} - \mathbf{w}_{j,s}) ds \\ & + \tau_i \gamma \int_0^t \left(\frac{\sigma_b}{\sigma_i} I + \mathbf{X}_i^\top \Omega_i^{-1} \right) dB_{i,s} + \varsigma \gamma \int_0^t \mathbf{X}_i^\top \Omega_i^{-1} \Lambda_i dB_s. \end{aligned}$$

Taking the derivative of the above equation, we get (10) with $g_{i,t} := \mathbf{X}_i^\top \Omega_i^{-1} \mathbf{X}_i (\mathbf{w}_{i,t} - \mathbf{w}^*)$, and $r_{i,t} := \sum_{j \neq i} \alpha_{i,j} (\mathbf{w}_{i,t} - \mathbf{w}_{j,t}) / \text{tr}(\Omega_j)$.

5.2.2 Approximation with noise from general distributions

Let the individual noise ε_i 's and the gradient error (if applicable) follow a distribution of expected value $\mathbf{0}$ and covariance matrix $\sigma_i^2 \mathbf{I}$ and $\sigma_b^2 \mathbf{I}$ receptively. The common noise follows a distribution with zero mean and identity covariance. We assume that the noise vectors and the gradient error are independent and identically distributed. We can see $\sum_{\Gamma l < t} \xi_l / n_t$, $\sum_{\Gamma l < t} \varepsilon_{i,l} / n_t$, and $\sum_{\Gamma l < t} \epsilon_{i,l} / n_t$ as the average of sequences of i.i.d. random variables. For all $i \in \mathcal{V}$ and $q \in \mathcal{D}$, by the Central Limit Theorem,

$$\frac{\sum_{\Gamma l < t} \varepsilon_{i,l}^{(q)}}{\sqrt{n_t}} \sim \mathcal{N}(0, \sigma_i^2), \quad \frac{\sum_{\Gamma l < t} \xi_l^{(q)}}{\sqrt{n_t}} \sim \mathcal{N}(0, 1), \quad \text{and} \quad \frac{\sum_{\Gamma l < t} \epsilon_{i,l}^{(q)}}{\sqrt{n_t}} \sim \mathcal{N}(0, \sigma_b^2).$$

It also follows that

$$\text{Var}\left[\Gamma \sqrt{n_t} \frac{\sum_{\Gamma l < t} \xi_l^{(q)}}{\sqrt{n_t}}\right] = \gamma \Gamma t, \quad \text{Var}\left[\Gamma \sqrt{n_t} \frac{\sum_{\Gamma l < t} \varepsilon_{i,l}^{(q)}}{\sqrt{n_t}}\right] = \gamma \Gamma \sigma_i^2 t,$$

$$\text{and } \text{Var} \left[\Gamma \sqrt{n_t} \frac{\sum_{\Gamma l < t} \epsilon_{i,l}^{(q)}}{\sqrt{n_t}} \right] = \gamma \Gamma \sigma_b^2 t.$$

Thus we would have the same noise Brownian approximation as in (29), (30), and (31), and the rest of steps follow as in (5.2.1). Hence we showed the continuous representation of $\mathbf{w}_{i,t}$ dynamics with general noise distribution.

5.3 Proof of Theorem 1

5.3.1 The differential form of the regularity measure

The following lemma provides the differential form of the regularity measure. We apply the Ito's lemma (Lemma 3) to $dV_{i,t}$ and then take the weighted average of $dV_{i,t}$'s to obtain $d\bar{V}_t$.

Lemma 4. *The regularity measure \bar{V}_t satisfies*

$$d\bar{V}_t = -\frac{\gamma}{v} \sum_{i=1}^N \frac{1}{\text{tr}(\Omega_i)} g_{i,t}^\top \mathbf{e}_{i,t} dt - \frac{\lambda\gamma}{v} \sum_{i=1}^N \frac{1}{\text{tr}(\Omega_i)} r_{i,t}^\top \mathbf{e}_{i,t} dt + \gamma K_1 d\tilde{B}_t + \gamma^2 C_1 dt, \quad (33)$$

where C_1 is the summation of constant terms,

$$C_1 = \frac{1}{2v} \sum_{i=1}^N \frac{1}{\text{tr}(\Omega_i)} C_{1,i}, \quad (34)$$

with $C_{1,i}$ for $i \in \mathcal{V}$ defined as,

$$\begin{aligned} C_{1,i} = & \tau_i^2 \left(1 - \frac{2}{v \text{tr}(\Omega_i)} \right) \left\| \frac{\sigma_b}{\sigma_i} I + \mathbf{X}_i^\top \Omega_i^{-1} \right\|_F^2 + \frac{1}{v^2} \sum_{k=1}^N \frac{\tau_k^2}{\text{tr}(\Omega_k)^2} \left\| \frac{\sigma_b}{\sigma_k} I + \mathbf{X}_k^\top \Omega_k^{-1} \right\|_F^2 \\ & + \varsigma^2 \left\| \mathbf{X}_i \Omega_i^{-1} \Lambda_i \right\|_F^2 + \frac{\varsigma^2}{v^2} \sum_{k=1}^N \sum_{j=1}^N \frac{1}{\text{tr}(\Omega_k) \text{tr}(\Omega_j)} \mathbf{1}^\top (\mathbf{X}_k^\top \Omega_k^{-1} \Lambda_k \circ \mathbf{X}_j^\top \Omega_j^{-1} \Lambda_j) \mathbf{1} \\ & - \frac{2\varsigma^2}{v} \sum_{k=1}^N \frac{1}{\text{tr}(\Omega_k)} \mathbf{1}^\top (\mathbf{X}_i^\top \Omega_i^{-1} \Lambda_i \circ \mathbf{X}_k^\top \Omega_k^{-1} \Lambda_k) \mathbf{1}, \end{aligned} \quad (35)$$

and $K_1 d\tilde{B}_t$ is the summation of Ito terms,

$$K_1 \tilde{B}_t = \frac{1}{v} \sum_{i=1}^N \frac{1}{\text{tr}(\Omega_i)} K_{1,i} d\tilde{B}_t, \quad (36)$$

with $K_{1,i} d\tilde{B}_t$ for $i \in \mathcal{V}$ defined as,

$$K_{1,i} d\tilde{B}_t = \varsigma \mathbf{X}_i^\top \Omega_i^{-1} \Lambda_i dB_t^\top \mathbf{e}_{i,t} + \tau_i \left(\frac{\sigma_b}{\sigma_i} I + \mathbf{X}_i^\top \Omega_i^{-1} \right) dB_{i,t}^\top \mathbf{e}_{i,t}. \quad (37)$$

Proof. By definition of $\hat{\mathbf{w}}_t$, we take the weighted average of (10) and obtain

$$\begin{aligned} d\hat{\mathbf{w}}_t = & -\frac{\gamma}{v} \sum_{k=1}^N \frac{1}{\text{tr}(\Omega_k)} g_{k,t} dt - \frac{\lambda\gamma}{v} \sum_{k=1}^N \frac{1}{\text{tr}(\Omega_k)} r_{k,t} dt + \frac{\gamma}{v} \sum_{k=1}^N \frac{\tau_k}{\text{tr}(\Omega_k)} \left(\frac{\sigma_b}{\sigma_i} I + \mathbf{X}_k^\top \Omega_k^{-1} \right) dB_{k,t} \\ & + \frac{\varsigma\gamma}{v} \sum_{k=1}^N \frac{1}{\text{tr}(\Omega_k)} \mathbf{X}_k^\top \Omega_k^{-1} \Lambda_k dB_t. \end{aligned} \quad (38)$$

We subtract (38) from (10), and by definition of $\mathbf{e}_{i,t}$, it follows that

$$\begin{aligned}
d\mathbf{e}_{i,t} &= d\mathbf{w}_{i,t} - d\hat{\mathbf{w}}_t \\
&= \gamma \left(-g_{i,t} + \frac{1}{v} \sum_{k=1}^N \frac{1}{\text{tr}(\Omega_k)} g_{k,t} \right) dt + \lambda \gamma \left(-r_{i,t} + \frac{1}{v} \sum_{k=1}^N \frac{1}{\text{tr}(\Omega_k)} r_{k,t} \right) dt \\
&\quad + \gamma \left(\tau_i \left(\frac{\sigma_b}{\sigma_i} I + \mathbf{X}_i^\top \Omega_i^{-1} \right) dB_{i,t} - \frac{1}{v} \sum_{k=1}^N \frac{\tau_k}{\text{tr}(\Omega_k)} \left(\frac{\sigma_b}{\sigma_k} I + \mathbf{X}_k^\top \Omega_k^{-1} \right) dB_{k,t} \right) \\
&\quad + \varsigma \gamma \left(\mathbf{X}_i^\top \Omega_i^{-1} \Lambda_i - \frac{1}{v} \sum_{k=1}^N \frac{1}{\text{tr}(\Omega_k)} \mathbf{X}_k^\top \Omega_k^{-1} \Lambda_k \right) dB_t.
\end{aligned} \tag{39}$$

Note that for d -by- m matrices $C = [c_1, \dots, c_d]$ and $Q = [q_1, \dots, q_d]$, $C dB_t \cdot C dB_t = \|C\|_F^2 dt$, and $C dB_t \cdot Q dB_t = \mathbf{1}^\top (C \circ Q) \mathbf{1}$, where “ $\mathbf{1}$ ” is a vector of all ones and “ \circ ” denotes the Hadamard product. Then by (39), the inner product of two $d\mathbf{e}_{i,t}$ is

$$d\mathbf{e}_{i,t} \cdot d\mathbf{e}_{i,t} = C_{1,i} \gamma^2 dt. \tag{40}$$

Apply Ito's lemma to $dV_{i,t}$, and by (40), we can obtain

$$\begin{aligned}
dV_{i,t} &= \mathbf{e}_{i,t} \cdot d\mathbf{e}_{i,t} + \frac{1}{2} d\mathbf{e}_{i,t} \cdot d\mathbf{e}_{i,t} \\
&= \gamma \left(-g_{i,t} + \frac{1}{v} \sum_{k=1}^N \frac{1}{\text{tr}(\Omega_k)} g_{k,t} \right)^\top \mathbf{e}_{i,t} dt + \gamma \lambda \left(-r_{i,t} + \frac{1}{v} \sum_{k=1}^N \frac{1}{\text{tr}(\Omega_k)} r_{k,t} \right)^\top \mathbf{e}_{i,t} dt \\
&\quad + \frac{\gamma^2}{2} C_{1,i} dt + \gamma K_{1,i} d\tilde{B}_t - \gamma K_1 \tilde{B}_t.
\end{aligned} \tag{41}$$

To obtain the differential form of the regularity measure, we take the weighted average of (41). Because of (18), the terms with double summation (weighting) vanish, and (33) follows.

5.3.2 Proof of Theorem 1

In the following proof, we first obtain an upper bound of $d\bar{V}_t$ given in (33) using the μ -Lipschitz continuity of the gradient g_i and the properties of the Laplacian matrix. Second, we integrate and take the expectation of the obtained bound to get the desired result.

Consider the first term of (33), let $h_t = \min_{i \in \mathcal{V}} g_{i,t}(\hat{\mathbf{w}}_t)$. By (18), we can add a zero-valued term $(h_t^\top / v) \sum_{i=1}^N \mathbf{e}_{i,t} / \text{tr}(\Omega_i)$ to the equation, and by the strong convexity of g_i (15), we can obtain the following inequality,

$$\begin{aligned}
-\frac{1}{v} \sum_{i=1}^N \frac{1}{\text{tr}(\Omega_i)} g_{i,t}^\top \mathbf{e}_{i,t} &= -\frac{1}{v} \sum_{i=1}^N \frac{1}{\text{tr}(\Omega_i)} (g_{i,t} - h_t)^\top \mathbf{e}_{i,t} \leq -\frac{1}{v} \sum_{i=1}^N \frac{1}{\text{tr}(\Omega_i)} (g_{i,t} - g_{i,t}(\hat{\mathbf{w}}_t))^\top \mathbf{e}_{i,t} \\
&\leq -\kappa \frac{1}{v} \sum_{i=1}^N \frac{\|\mathbf{e}_{i,t}\|^2}{\text{tr}(\Omega_i)} = -2\kappa \bar{V}_t.
\end{aligned} \tag{42}$$

The first inequality above follows from the definition of h_t , and the second inequality is by the strict convexity of the gradient g_i .

Now we consider the second term of (33). Define the vector $\mathbf{e}_t = [\mathbf{e}_{1,t}^T, \dots, \mathbf{e}_{N,t}^T]^T$ and the matrix $\hat{L} = L \otimes I_m$, where \otimes is the Kronecker product. Using these definitions, we can express (43) as follows,

$$-\sum_{i=1}^N \frac{1}{\text{tr}(\Omega_i)} \sum_{j=1, j \neq i}^N \frac{\alpha_{ij}}{\text{tr}(\Omega_j)} (\mathbf{w}_{i,t} - \mathbf{w}_{j,t})^T \mathbf{e}_{i,t} = \sum_{i=1}^N \sum_{j \neq i}^N \frac{-\alpha_{ij}}{\text{tr}(\Omega_i) \text{tr}(\Omega_j)} (\mathbf{e}_{i,t} - \mathbf{e}_{j,t})^T \mathbf{e}_{i,t} = -\mathbf{e}_t^T \hat{L} \mathbf{e}_t, \quad (43)$$

where the first equality follows by adding and subtracting $\hat{\mathbf{w}}_t$ and the second equality is by the definition of \hat{L} . Note that the second largest eigenvalue a_2 satisfies $\min_{x \neq 0, 1^T x = 0} (x^T L x) / \|x\|^2 = a_2$ [27]. Thus, we have

$$-\mathbf{e}_t^T \hat{L} \mathbf{e}_t \leq -a_2 \sum_{i=1}^N \|\mathbf{e}_{i,t}\|^2. \quad (44)$$

Combining (43) and (44), we have the following,

$$\begin{aligned} -\frac{\lambda\gamma}{v} \sum_{i=1}^N \frac{1}{\text{tr}(\Omega_i)} r_{i,t}^T \mathbf{e}_{i,t} &\leq -\lambda\gamma a_2 \sum_{i=1}^N \|\mathbf{e}_{i,t}\|^2 \\ &\leq -2\lambda\gamma a_2 \frac{1}{v} \sum_{i=1}^N \frac{V_{i,t}}{\text{tr}(\Omega_i)} = -2\lambda\gamma a_2 \bar{V}_t. \end{aligned} \quad (45)$$

The second inequality follows since the left-hand side is a sum and the right-hand side is the weighted average, and the final equality is by the definition of \bar{V}_t . An upper bound for $d\bar{V}_t$ follows from (42) and (45),

$$d\bar{V}_t \leq -2\gamma(\kappa + \lambda a_2) \bar{V}_t dt + \gamma^2 C_1 dt + \gamma K_1 d\tilde{B}_t \quad (46)$$

Now consider the derivative of $e^{2(\kappa + \lambda a_2)\gamma t} \bar{V}_t$,

$$\begin{aligned} d(e^{2(\kappa + \lambda a_2)\gamma t} \bar{V}_t) &= e^{2(\kappa + \lambda a_2)\gamma t} d\bar{V}_t + 2(\kappa + \lambda a_2)\gamma e^{2(\kappa + \lambda a_2)\gamma t} \bar{V}_t dt \\ &\leq e^{2(\kappa + \lambda a_2)\gamma t} \gamma^2 C_1 dt + e^{2(\kappa + \lambda a_2)\gamma t} \gamma K_1 d\tilde{B}_t, \end{aligned} \quad (47)$$

where the inequality follows by using (46) for each $d\bar{V}_t$ term. Integrating both sides of the inequality in (47),

$$\bar{V}_t \leq e^{-2(\kappa + \lambda a_2)\gamma t} \bar{V}_0 + \frac{\gamma C_1}{2(\kappa + \lambda a_2)} (1 - e^{-2(\kappa + \lambda a_2)\gamma t}) + e^{-2(\kappa + \lambda a_2)\gamma t} \int_0^t e^{2(\kappa + \lambda a_2)\gamma s} K_1 d\tilde{B}_s. \quad (48)$$

Since the stochastic integral is a martingale,

$$E\left[\int_0^t e^{2(\kappa + \lambda a_2)\gamma s} K_1 d\tilde{B}_s\right] = 0.$$

We obtain the desired upper bound by taking the expectation on both sides of (48). In the long run, as $t \rightarrow \infty$, the exponential terms will vanish, and the upper bound of the regularity measure follows.

5.4 Proof of Theorem 2

The proof follows a similar outline as Theorem 1. We start with Ito's Lemma to get the stochastic dynamics form of dU_t and then introduce an auxiliary variable W_t that depends on both U_t and \bar{V}_t to bound $E[U_t]$.

We apply Ito's lemma to dU_t , and use the identity in (18) and the differential form of \mathbf{w}_t in (38) to get the following form,

$$\begin{aligned}
dU_t &= (\hat{\mathbf{w}}_t - \mathbf{w}^*) \cdot d(\hat{\mathbf{w}}_t - \mathbf{w}^*) + \frac{1}{2} d(\hat{\mathbf{w}}_t - \mathbf{w}^*) \cdot d(\hat{\mathbf{w}}_t - \mathbf{w}^*) \\
&= -\frac{\gamma}{v} \sum_{k=1}^N \frac{1}{\text{tr}(\Omega_k)} g_{k,t}^\top (\hat{\mathbf{w}}_t - \mathbf{w}^*) dt + \frac{\gamma}{v} \sum_{k=1}^N \frac{\tau_k}{\text{tr}(\Omega_k)} \left(\left(\frac{\sigma_b}{\sigma_i} I + \mathbf{X}_k^\top \Omega_k^{-1} \right) dB_{k,t} \right)^\top (\hat{\mathbf{w}}_t - \mathbf{w}^*) \\
&\quad + \frac{\varsigma \gamma}{v} \sum_{k=1}^N \frac{1}{\text{tr}(\Omega_k)} (\mathbf{X}_k^\top \Omega_k^{-1} \Lambda_k dB_t)^\top (\hat{\mathbf{w}}_t - \mathbf{w}^*) + \frac{\gamma^2}{2v^2} \left(\sum_{k=1}^N \frac{\tau_k^2}{\text{tr}(\Omega_k)^2} \|\mathbf{X}_k \Omega_k^{-1}\|_F^2 + \right. \\
&\quad \left. \varsigma^2 \sum_{k=1}^N \sum_{j=1}^N \frac{1}{\text{tr}(\Omega_k) \text{tr}(\Omega_j)} \mathbf{1}^\top (\mathbf{X}_k^\top \Omega_k^{-1} \Lambda_k \circ \mathbf{X}_j^\top \Omega_j^{-1} \Lambda_j) \mathbf{1} \right) dt
\end{aligned} \tag{49}$$

We separate the first term of (49) using the identity $\hat{\mathbf{w}}_t - \mathbf{w}^* = (\mathbf{w}_{k,t} - \mathbf{w}^*) - \mathbf{e}_{k,t}$, and rearrange constant and Ito terms to get

$$dU_t = -\frac{\gamma}{v} \sum_{k=1}^N \frac{1}{\text{tr}(\Omega_k)} g_{k,t}^\top (\mathbf{w}_{k,t} - \mathbf{w}^*) dt + \frac{\gamma}{v} \sum_{k=1}^N \frac{1}{\text{tr}(\Omega_k)} g_{k,t}^\top e_{k,t} dt + K_2 d\tilde{B}_t + \gamma^2 C_2 dt \tag{50}$$

where the summation term C_2 is defined in (19) and $K_2 d\tilde{B}_t$ is given as,

$$K_2 d\tilde{B}_t = \frac{\gamma}{v} \sum_{k=1}^N \frac{\tau_k}{\text{tr}(\Omega_k)} (\hat{\mathbf{w}}_t - \mathbf{w}^*)^\top \left(\frac{\sigma_b}{\sigma_i} I + \mathbf{X}_k^\top \Omega_k^{-1} \right) dB_{k,t} + \frac{\varsigma \gamma}{v} \sum_{k=1}^N \frac{1}{\text{tr}(\Omega_k)} (\hat{\mathbf{w}}_t - \mathbf{w}^*)^\top \mathbf{X}_k^\top \Omega_k^{-1} \Lambda_k dB_t.$$

We have the following upper bound on the first term of (50),

$$\begin{aligned}
&-\frac{\gamma}{v} \sum_{k=1}^N \frac{1}{\text{tr}(\Omega_k)} g_{k,t}^\top (\mathbf{w}_{k,t} - \mathbf{w}^*) = -\frac{\gamma}{v} \sum_{k=1}^N \frac{1}{\text{tr}(\Omega_k)} (g_{k,t} - g(\mathbf{w}^*))^\top (\mathbf{w}_{k,t} - \mathbf{w}^*) \\
&\leq -\frac{2\kappa\gamma}{v} \sum_{k=1}^N \frac{1}{2\text{tr}(\Omega_k)} \|\mathbf{w}_{k,t} - \hat{\mathbf{w}}_t + \hat{\mathbf{w}}_t - \mathbf{w}^*\|^2 = -2\kappa\gamma(\bar{V}_t + U_t).
\end{aligned} \tag{51}$$

The first equality is obtained by subtracting the zero-valued term $g(\mathbf{w}^*)$ from $g_{k,t}$. The second inequality is by strong convexity of the gradients $(g_{k,t})$, and the last equality follows from (16).

Now consider the second term of (50). Let $q_t = \max_{k \in \mathcal{V}} g_k(\hat{\mathbf{w}}_t)$, then it follows that

$$\frac{\gamma}{v} \sum_{k=1}^N \frac{1}{\text{tr}(\Omega_k)} g_{k,t}^\top e_{k,t} = \frac{\gamma}{v} \sum_{k=1}^N \frac{1}{\text{tr}(\Omega_k)} (g_{k,t} - q_t)^\top e_{k,t} \leq \frac{2\gamma}{v} \sum_{k=1}^N \frac{1}{2\text{tr}(\Omega_k)} (g_{k,t} - g_k(\hat{\mathbf{w}}_t))^\top e_{k,t} \leq 2\mu\gamma\bar{V}_t. \tag{52}$$

The equality is obtained by subtracting the zero-valued term $(q_t\gamma/v) \sum_{k=1}^N \mathbf{e}_{k,t} / \|\Lambda_k\|_F^2$. The first inequality follows by the definition of q_t , and the second inequality is by the Lipschitz continuity of $g_{k,t}$'s.

By (50)–(52), we can obtain an upper bound of dU_t ,

$$dU_t \leq -2\kappa\gamma U_t dt + 2\gamma(\mu - \kappa)\bar{V}_t dt + \gamma^2 C_2 dt + K_2 d\tilde{B}_t. \quad (53)$$

We construct an auxiliary variable W_t and then follow similar steps as in the proof of Theorem 1: integrate the upper bound of dW_t and then take expectation. Now, define

$$W_t = U_t + \frac{\mu - \kappa}{\lambda a_2} \bar{V}_t.$$

The differential of W_t can be obtained as follows,

$$\begin{aligned} dW_t &\leq -2\kappa\gamma U_t dt + \left(2(\mu - \kappa)\gamma\bar{V}_t + \gamma^2 C_2\right) dt \\ &\quad + K_2 d\tilde{B}_t + \frac{\mu - \kappa}{\lambda a_2} \left(-2\lambda a_2 \gamma \bar{V}_t dt - 2\kappa\gamma \bar{V}_t dt + \gamma K_1 d\tilde{B}_t + \gamma^2 C_1 dt\right) \\ &= -2\kappa\gamma U_t dt - 2\kappa\gamma \frac{\mu - \kappa}{\lambda a_2} (\lambda a_2 + \kappa) \bar{V}_t dt + \\ &\quad \gamma^2 \left(\frac{\mu - \kappa}{\lambda a_2} C_1 + C_2\right) dt + \left(\frac{\gamma(\mu - \kappa)}{\lambda a_2} K_1 + K_2\right) d\tilde{B}_t \\ &= -2\kappa\gamma W_t dt + \gamma^2 \left(\frac{\mu - \kappa}{\lambda a_2} C_1 + C_2\right) dt + \left(\frac{\gamma(\mu - \kappa)}{\lambda a_2} K_1 + K_2\right) d\tilde{B}_t. \end{aligned} \quad (54)$$

The inequality is obtained by plugging in the bounds for $d\bar{V}_t$ in (46) and for dU_t in (53) into dW_t . The first equality follows by rearranging terms, and the second one is obtained by combining terms that are equivalent to W_t .

Consider the derivative of $e^{2\kappa\gamma t} W_t$ and plug in the upper bound of dW_t in (54) to obtain,

$$\begin{aligned} d(e^{2\kappa\gamma t} W_t) &= e^{2\kappa\gamma t} dW_t + 2\kappa\gamma e^{2\kappa\gamma t} W_t dt \\ &\leq e^{2\kappa\gamma t} \gamma^2 \left(\frac{\mu - \kappa}{\lambda a_2} C_1 + C_2\right) dt + e^{2\kappa\gamma t} \left(\frac{\gamma(\mu - \kappa)}{\lambda a_2} K_1 + K_2\right) d\tilde{B}_t \end{aligned} \quad (55)$$

The following inequality is obtained by integrating both sides of (55),

$$\begin{aligned} W_t &\leq e^{-2\kappa\gamma t} W_0 + \int_0^t e^{2\kappa\gamma s} \gamma^2 \left(\frac{\mu - \kappa}{\lambda a_2} C_1 + C_2\right) ds + \int_0^t e^{2\kappa\gamma s} \left(\frac{\gamma(\mu - \kappa)}{\lambda a_2} K_1 + K_2\right) d\tilde{B}_s \\ &= e^{-2\kappa\gamma t} W_0 + \frac{\gamma}{2\kappa} \left(\frac{\mu - \kappa}{\lambda a_2} C_1 + C_2\right) (1 - e^{-2\kappa\gamma t}) + \int_0^t e^{2\kappa\gamma s} \left(\frac{\gamma(\mu - \kappa)}{\lambda a_2} K_1 + K_2\right) d\tilde{B}_s. \end{aligned} \quad (56)$$

We assume that all nodes have the same initial estimate, i.e., $\mathbf{w}_{i,0} = \mathbf{w}_{j,0}$ for all i, j . Then, $\bar{V}_0 = 0$, which means $W_0 = U_0$. Note that the stochastic integration of the Ito term is martingale and hence the expectation is zero. Taking expectation on both sides of (56), then

$$\mathbb{E}[W_t] \leq e^{-2\kappa\gamma t} U_0 + \frac{\gamma}{2\kappa} \left(\frac{\mu - \kappa}{\lambda a_2} C_1 + C_2\right) (1 - e^{-2\kappa\gamma t}). \quad (57)$$

Since $\mu - \kappa > 0$, we have

$$\mathbb{E}[U_t] \leq \mathbb{E}[W_t].$$

Hence the right-hand side of (57) is also the upper bound of $\mathbb{E}[U_t]$. In the long run, as $t \rightarrow \infty$, the exponential terms vanish and the upper bound of the consistency measure follows.

5.5 Proof of Lemma 2

We will find upper bounds for (20), or more specifically, upper bounds for the constants term $C_1/\lambda a_2$ (defined in (34)-(35)) and C_2 (defined in (19)), and further prove that these bounds are functions of Γ and can be controlled as small as needed. With a slight abuse of notation, we refer to N as the total number of nodes.

By hypothesis, $0 < \epsilon \leq \sigma_i^2$ and $\text{tr}(\Omega_i) \leq M$, for all $i \in \mathcal{V}$. By choosing $\lambda a_2 \sim N$ (i.e., network connectivity is preserved) and $\Gamma \sim \epsilon^4$, we prove that the difference between the ensemble average estimate and the ground truth is $O(\Gamma^{1/4})$ as $N \rightarrow \infty$. We start by discussing the bound for C_2 and then use the results to construct the bound for $C_1/\lambda a_2$. For notational simplicity, we substitute λa_2 by N in the following discussion.

5.5.1 Limiting property of C_2

Consider the first summation term of C_2 inside the parentheses. For $i \in \mathcal{V}$, rewrite the data subsets and the matrices as $X_i^\top = [\mathbf{x}_{i,1}, \dots, \mathbf{x}_{i,m}]$ and $\Lambda_i = \text{diag}(\omega_{i,1}, \dots, \omega_{i,m})$, then

$$\begin{aligned} \frac{\tau_i^2}{\text{tr}(\Omega_i)^2} \|\mathbf{X}_i \Omega_i^{-1}\|_F^2 &= \frac{\sigma_i^2 \Gamma \Delta t}{\text{tr}(\Omega_i)^2} \|\mathbf{X}_i \Omega_i^{-1}\|_F^2 < m x_m^2 \sum_{k=1}^m \frac{1}{(\sigma_i^2 + \omega_{i,k}^2)^2} \frac{\sigma_i^2 \Gamma \Delta t}{(m \sigma_i^2 + \sum_{k=1}^m \omega_{i,k}^2)^2} \\ &< \frac{x_m^2 \Gamma \Delta t}{\epsilon^3} \triangleq S_1(\epsilon) \end{aligned}$$

where x_m is the largest element among the data matrix X . The first inequality is obtained by substituting matrix X by its extreme values $x_m I$, and the second inequality follows by eliminating $\sum_{k=1}^m \omega_{i,k}^2$ of the denominator. Then

$$\frac{1}{v^2} \sum_{i=1}^N \frac{\tau_i^2}{\text{tr}(\Omega_i)^2} \|\mathbf{X}_i \Omega_i^{-1}\|_F^2 < \frac{S_1(\epsilon) N}{\left(\sum_{i=1}^N \frac{1}{\text{tr}(\Omega_i)}\right)^2} \leq \frac{S_1(\epsilon) M^2}{N}. \quad (58)$$

Since $S_1(\epsilon) M^2$ is $O(\Gamma^{1/4})$, then $\lim_{N \rightarrow \infty} S_1(\epsilon) M^2 / N = 0$.

Now consider the second term of C_2 , we observe that

$$\mathbf{X}_i^\top \Omega_i^{-1} \Lambda_i \circ \mathbf{X}_j^\top \Omega_j^{-1} \Lambda_j = [\omega_{i,1} \omega_{j,1} c_{i,j,1} \mathbf{x}_{i,1} \circ \mathbf{x}_{j,1}, \dots, \omega_{i,m} \omega_{j,m} c_{i,j,m} \mathbf{x}_{i,m} \circ \mathbf{x}_{j,m}],$$

where

$$c_{i,j,k} = \frac{1}{(\sigma_i^2 + \omega_{i,k}^2)(\sigma_j^2 + \omega_{j,k}^2)}.$$

Note that $\mathbf{1}^\top(\mathbf{x}_{i,k} \circ \mathbf{x}_{j,k}) = \mathbf{x}_{i,k}^\top \mathbf{x}_{j,k}$, we set $S_2 = \max_{k,j} \max_i \mathbf{x}_{i,k}^\top \mathbf{x}_{j,k}$. By substituting the terms with their extreme values and the Cauchy-Schwarz inequality, we can obtain

$$\begin{aligned} \mathbf{1}^\top(\mathbf{X}_i^\top \Omega_i^{-1} \Lambda_i \circ \mathbf{X}_j^\top \Omega_j^{-1} \Lambda_j) \mathbf{1} &= S_2 \sum_{k=1}^m \frac{\omega_{i,k} \omega_{j,k}}{(\sigma_i^2 + \omega_{i,k}^2)(\sigma_j^2 + \omega_{j,k}^2)} < S_2 \sum_{k=1}^m \frac{\omega_{i,k} \omega_{j,k}}{\sigma_i^2 \sigma_j^2} \\ &< \frac{S_2}{\epsilon^2} \sum_{k=1}^m \omega_{i,k} \omega_{j,k} = \frac{S_2}{\epsilon^2} \|\Lambda_i \Lambda_j\|_F \leq \frac{S_2}{\epsilon^2} \|\Lambda_i\|_F \|\Lambda_j\|_F. \end{aligned}$$

Note that $\|\Lambda_i\|_F \leq \sqrt{\text{tr}(\Omega_i)}$, it follows that

$$\begin{aligned} & \frac{\varsigma^2}{v^2} \sum_{k=1}^N \sum_{j=1}^N \frac{1}{\text{tr}(\Omega_k) \text{tr}(\Omega_j)} \mathbf{1}^\top (\mathbf{X}_k^\top \Omega_k^{-1} \Lambda_k \circ \mathbf{X}_j^\top \Omega_j^{-1} \Lambda_j) \mathbf{1} \leq \frac{S_2 \Gamma \Delta t}{\epsilon^2 v^2} \left(\sum_{i=1}^N \frac{1}{\sqrt{\text{tr}(\Omega_i)}} \right)^2 \\ & = \frac{S_2 \Gamma \Delta t}{\epsilon^2} \left(\frac{\sum_{i=1}^N \frac{1}{\sqrt{\text{tr}(\Omega_i)}}}{\sum_{i=1}^N \frac{1}{\text{tr}(\Omega_i)}} \right)^2 < \frac{S_2 M^2 \Gamma \Delta t}{m \epsilon^3} = O(\Gamma^{1/4}). \end{aligned} \quad (59)$$

By (58) and (59), we say that C_2 is upper bounded by $O(\Gamma^{1/4})$.

5.5.2 Limiting property of C_1

Now consider C_1/N . As C_1 (defined in (34)) is the weighted average of $C_{1,i}$'s (defined in (35)), we only need to discuss the limiting property of $C_{1,i}$.

Consider the first term of $C_{1,i}$,

$$\begin{aligned} & \tau_i^2 \left(1 - \frac{2}{v \text{tr}(\Omega_i)^2} \right) \left\| \frac{\sigma_b}{\sigma_i} I + \mathbf{X}_i \Omega_i^{-1} \right\|_F^2 < \tau_i^2 \left(\left\| \frac{\sigma_b}{\sigma_i} I \right\|_F + \|\mathbf{X}_i \Omega_i^{-1}\|_F \right)^2 \\ & < m \Gamma \Delta t \sigma_i^2 \left(\frac{\sigma_b^2}{\sigma_i^2} + x_m^2 \sum_{k=1}^m \frac{1}{(\sigma_i^2 + \omega_{i,k}^2)^2} + 2x_m \frac{\sigma_b}{\sigma_i} \sqrt{\sum_{k=1}^m \frac{1}{(\sigma_i^2 + \omega_{i,k}^2)^2}} \right) \\ & < m \Gamma \Delta t \left(\sigma_b^2 + \frac{x_m^2 m}{\epsilon} + \frac{2x_m m^{1/2} \sigma_b}{\sqrt{\epsilon}} \right) \triangleq S_3(\epsilon). \end{aligned} \quad (60)$$

The first line is obtained by the triangle inequality, and the second follows by eliminating $\omega_{i,k}^2$ terms from the denominators. Note that $S_3(\epsilon) = O(\Gamma^{3/4})$, and it follows that $\lim_{N \rightarrow \infty} S_3(\epsilon)/N = 0$.

Now look at the second term of $C_{1,i}$, by triangle inequality, we can obtain

$$\begin{aligned} & \frac{1}{v^2} \sum_{k=1}^N \frac{\tau_k^2}{\text{tr}(\Omega_k)^2} \left\| \frac{\sigma_b}{\sigma_k} I + \mathbf{X}_k^\top \Omega_k^{-1} \right\|_F^2 < \frac{1}{v^2} \sum_{k=1}^N \frac{m \tau_k^2}{\text{tr}(\Omega_k)^2} \frac{\sigma_b^2}{\sigma_k^2} + \frac{1}{v^2} \sum_{k=1}^N \frac{\tau_k^2}{\text{tr}(\Omega_k)^2} \|\mathbf{X}_k^\top \Omega_k^{-1}\|_F^2 \\ & \quad + \frac{1}{v^2} \sum_{k=1}^N \frac{2x_m m \tau_k^2}{\text{tr}(\Omega_k)^2} \frac{\sigma_b}{\sigma_k} \sqrt{\sum_{l=1}^m \frac{1}{(\sigma_k^2 + \omega_{k,l}^2)^2}} \end{aligned} \quad (61)$$

The second part of (61) is the same as (58), which goes to zero as $N \rightarrow \infty$, and the first part is as following:

$$\frac{m \tau_k^2}{\text{tr}(\Omega_k)^2} \frac{\sigma_b^2}{\sigma_k^2} = \frac{m \sigma_b^2 \Gamma \Delta t}{(m \sigma_i^2 + \sum_{k=1}^m \omega_{i,k}^2)^2} < \frac{\sigma_b^2 \Gamma \Delta t}{m \epsilon^2} \triangleq S_4(\epsilon).$$

Note that $S_4(\epsilon) = O(\Gamma^{1/2})$, then it follows that

$$\frac{1}{v^2} \sum_{k=1}^N \frac{m \tau_k^2}{\text{tr}(\Omega_k)^2} \frac{\sigma_b^2}{\sigma_k^2} < \frac{S_4(\epsilon) N}{\left(\sum_{i=1}^N \frac{1}{\text{tr}(\Omega_i)} \right)^2} \leq \frac{S_4(\epsilon) M^2}{N}.$$

The third part third part is as following:

$$\begin{aligned} & \frac{1}{v^2} \sum_{k=1}^N \frac{2x_m m \tau_k^2}{\text{tr}(\Omega_k)^2} \frac{\sigma_b}{\sigma_k} \sqrt{\sum_{l=1}^m \frac{1}{(\sigma_k^2 + \omega_{k,l}^2)^2}} < \frac{1}{v^2} \sum_{k=1}^N \frac{2x_m m^{3/2} \sigma_b \Gamma \Delta t}{\text{tr}(\Omega_k)^2 \sigma_k} \\ & < \frac{2M^2 x_m \sigma_b \Gamma \Delta t}{m^{1/2} \epsilon^{5/2} N} = O(\Gamma^{3/8}) \end{aligned}$$

Note that When divided by N , it follows that

$$\lim_{N \rightarrow \infty} \frac{S_4(\epsilon) M^2}{N^2} = 0, \quad \text{and} \quad \lim_{N \rightarrow \infty} \frac{2M^2 x_m \sigma_b \Gamma \Delta t}{m^{1/2} \epsilon^{5/2} N^2} = 0.$$

Hence we conclude that

$$\lim_{N \rightarrow \infty} \frac{1}{v^2 N} \sum_{k=1}^N \frac{\tau_k^2}{\text{tr}(\Omega_k)^2} \left\| \frac{\sigma_b}{\sigma_k} I + \mathbf{X}_k^T \Omega_k^{-1} \right\|_F^2 = 0.$$

For the third part of C_1 , we observe that

$$\varsigma^2 \left\| \mathbf{X}_i \Omega_i^{-1} \Lambda_i \right\|_F^2 = m x_m^2 \Gamma \Delta t \sum_{k=1}^m \frac{\mathbf{w}_{i,k}^2}{(\sigma_i^2 + \mathbf{w}_{i,k}^2)^2} < \frac{m^2 x_m^2 \Gamma \Delta t M^2}{\epsilon^2} \triangleq S_5(\epsilon).$$

Since $S_5(\epsilon) = O(\Gamma^{1/2})$, we have $\lim_{N \rightarrow \infty} S_5(\epsilon)/N = 0$.

The fourth term of C_1 is the same as the second part of C_2 , which is upper bounded by $O(\Gamma^{1/4})$, then

$$\lim_{N \rightarrow \infty} \frac{S_2 M^2 \Gamma \Delta t}{m N \epsilon^3} = 0.$$

Finally, we consider the last part of C_1 . By (59),

$$\begin{aligned} \frac{2\varsigma^2}{v} \sum_{k=1}^N \frac{1}{\text{tr}(\Omega_k)} \mathbf{1}^T (\mathbf{X}_i^T \Omega_i^{-1} \Lambda_i \circ \mathbf{X}_k^T \Omega_k^{-1} \Lambda_k) \mathbf{1} & < \frac{2\varsigma^2 S_2 / \epsilon^2}{v} \sum_{k=1}^N \frac{1}{\text{tr}(\Omega_k)} \|\Lambda_i\|_F \|\Lambda_k\|_F \leq \frac{2N S_2 \sqrt{M} \Gamma \Delta t}{\epsilon^2 \sqrt{m} \epsilon \sum_{k=1}^N \frac{1}{\text{tr}(\Omega_k)}} \\ & \leq \frac{2S_2 M^{3/2} \Gamma \Delta t}{\epsilon^{5/2} \sqrt{m}} \triangleq S_6(\epsilon). \end{aligned}$$

Note that $S_6(\epsilon) = O(\Gamma^{3/8})$, then $\lim_{N \rightarrow \infty} S_6(\epsilon)/N = 0$.

Since all terms of C_1 go to zero when divided by N , we conclude that

$$\lim_{N \rightarrow \infty} \frac{C_1}{N} = 0 \tag{62}$$

5.5.3 Proof of consistency

By (58), (59), and (62), and when we choose $\lambda a_2 \sim N$ and $\Gamma \sim \epsilon^4$, then

$$\lim_{t \rightarrow \infty} \lim_{N \rightarrow \infty} \mathbb{E}[\|\hat{\mathbf{w}}_t - \mathbf{w}^*\|^2] = \lim_{t \rightarrow \infty} \lim_{N \rightarrow \infty} 2\mathbb{E}[U_t] \leq \frac{\gamma}{\kappa} \left(\frac{\mu - \kappa}{\lambda a_2} C_1 + C_2 \right) < \frac{S_2 M^2 \Gamma}{m \kappa \epsilon^3} = O(\Gamma^{1/4}),$$

where $S_2 = \max_{k,j} \max_i \mathbf{x}_{i,k}^T \mathbf{x}_{i,j}$.

References

- [1] Y. Zhang, J. Duchi, and M. Wainwright, “Divide and conquer kernel ridge regression: A distributed algorithm with minimax optimal rates,” *Journal of Machine Intelligence Research*, vol. 16, pp. 3299–3340, 2015.
- [2] J. Predd, S. Kulkarni, and H. V. Poor, “A collaborative training algorithm for distributed learning,” *IEEE Transactions on Information Theory*, vol. 55, pp. 1856–1869, 2009.
- [3] Y. Zhang, J. Duchi, and M. Wainwright, “Communication-efficient algorithms for statistical optimization,” *Journal of Machine Intelligence Research*, vol. 14, pp. 3321–3363, 2013.
- [4] B. Hansen, “Least squares model averaging,” *Econometrica*, vol. 75, no. 4, pp. 1175–1189, 2007.
- [5] Q. Liu, R. Okui, and A. Yoshimura, “Generalized least squares model averaging,” *Econometric Reviews*, vol. 35, no. 8, pp. 1692–1752, 2016.
- [6] J. Mendes-Moreira, C. Soares, A. Jorge, and J. Freire de Sousa, “Ensemble approaches for regression: A survey,” *ACM Computing Surveys*, vol. 45, no. 1, pp. 10–40, 2012.
- [7] J. M. Bates and C. M. W. Granger, “The combination of forecasts,” *Operations Research Quarterly*, vol. 20, pp. 451–468, 1969.
- [8] C. M. W. Granger and R. Ramanathan, “Improved methods of combining forecast accuracy,” *Journal of Forecasting*, vol. 19, pp. 197–204, 1984.
- [9] H. B. McMahan, E. Moore, D. Ramage, S. Hampson, *et al.*, “Communication-efficient learning of deep networks from decentralized data,” *arXiv preprint arXiv:1602.05629*, 2016.
- [10] J. Konecny, H. B. McMahan, F. X. Yu, P. Richtarik, A. T. Suresh, and D. Bacon, “Federated learning: Strategies for improving communication efficiency,” *arXiv preprint arXiv:1610.05492*, 2016.
- [11] V. Smith, C.-K. Chiang, M. Sanjabi, and A. S. Talwalkar, “Federated multi-task learning,” in *Advances in Neural Information Processing Systems*, pp. 4424–4434, 2017.
- [12] C. He, T. Xie, Y. Zhengyu, Z. Hu, and S. Xia, “Federated multi-task learning with decentralized periodic averaging sgd,” 2019.
- [13] D. Hallac, J. Leskovec, and S. Boyd, “Network lasso: Clustering and optimization in large graphs,” *Proceedings SIGKDD*, pp. 387–396, 2015.
- [14] A. Jung, T. Nguyen, and A. Mara, “When is network lasso accurate?,” *Frontiers in Applied Mathematics and Statistics*, vol. 3, pp. 1–11, 2018.
- [15] M. Yamada, T. Koh, T. Iwata, S.-T. J., and S. Kaski, “Localized lasso for high-dimensional regression,” *Conference on Artificial Intelligence and Statistics, AISTATS*, pp. 325–333, 2017.
- [16] J. Tsitsiklis, D. Bertsekas, and M. Athans, “Distributed asynchronous deterministic and stochastic gradient optimization algorithms,” *IEEE transactions on automatic control*, vol. 31, no. 9, pp. 803–812, 1986.

- [17] A. Nedic and A. Ozdaglar, “Distributed subgradient methods for multi-agent optimization,” *IEEE Transactions on Automatic Control*, vol. 54, no. 1, p. 48, 2009.
- [18] J. C. Duchi, A. Agarwal, and M. J. Wainwright, “Dual averaging for distributed optimization: Convergence analysis and network scaling,” *IEEE Transactions on Automatic control*, vol. 57, no. 3, pp. 592–606, 2011.
- [19] A. Mokhtari and A. Ribeiro, “Dsa: Decentralized double stochastic averaging gradient algorithm,” *The Journal of Machine Learning Research*, vol. 17, no. 1, pp. 2165–2199, 2016.
- [20] W. Shi, Q. Ling, G. Wu, and W. Yin, “Extra: An exact first-order algorithm for decentralized consensus optimization,” *SIAM Journal on Optimization*, vol. 25, no. 2, pp. 944–966, 2015.
- [21] L. He, A. Bian, and M. Jaggi, “Cola: Decentralized linear learning,” in *Advances in Neural Information Processing Systems*, pp. 4536–4546, 2018.
- [22] C. Eksin and A. Ribeiro, “Distributed network optimization with heuristic rational agents,” *IEEE Transactions on Signal Processing*, vol. 60, no. 10, pp. 5396–5411, 2012.
- [23] D. T. Blumstein, “Flight-initiation distance in birds is dependent on intruder starting distance,” *The Journal of Wildlife Management*, pp. 852–857, 2003.
- [24] F. Morelli, Y. Benedetti, M. Diaz, T. Grim, J. D. Ibanez-Alamo, J. Jokimaki, M.-L. Kisanlahti-Jokimaki, K. Tatte, G. Marko, Y. Jiang, *et al.*, “Contagious fear: Escape behavior increases with flock size in european gregarious birds,” *Ecology and evolution*, vol. 9, no. 10, pp. 6096–6104, 2019.
- [25] J. Nocedal and S. Wright, *Numerical optimization*. Springer Science & Business Media, 2006.
- [26] B. Oksendal, “Stochastic differential equations,” in *Stochastic differential equations*, pp. 65–84, Springer, 2003.
- [27] C. Godsil and G. Royle, “Algebraic graph theory,” *Springer, New York*, 2001.